Supplemental Information to:

RodZ (YfgA) is required for proper assembly of the MreB actin cytoskeleton and cell shape in *Escherichia coli*.

by

Felipe O. Bendezú, Cynthia A. Hale, Thomas G. Bernhardt, and Piet A.J. de Boer

Case Western Reserve University, School of Medicine, Department of Molecular Biology and Microbiology, Cleveland, OH 44106

Table S1. Division inhibition upon overproduction of MreB and/or RodZ.

[a]Plasmid(s)	[b]Protein	Medium	n	[c]Length	[c]Width	[e]Dividing
pJF188EH	-	LB	50	4.7	1.0	20
pFB216	MreB	LB	50	14.7	1.7	8
pFB291	RodZ	LB	50	8.4	1.3	14
pFB216+pFB291	MreB+RodZ	LB	20	59.1	[d]0.9	0
pJF188EH	-	M9	50	3.0	1.0	9
pFB216+pFB291	MreB+RodZ	M9	20	34.6	[d]0.8	0

[a]Strain FB83 [*mreB-rfp*^{sw}] harboring pJF188EH (the vector parent of pFB291), pFB216 [P_{tac}::*mreB*], pFB291[P_{tac}::*rodZ*], or both pFB216 and pFB291, were inoculated to OD_{600}=0.005 in LB or M9-mal supplemented with appropriate antibiotics and 250 μM IPTG. After growth at 30^{o}C to OD_{600}=0.5, cells were fixed and imaged with DIC.

[b]Overexpressed protein.

[c]Average vakues in μ.

[d]Width was measured at three well separated locations along the long axis, and values were averaged.

[e]number of cells with a clearly visible division septum.

Table S2. *E.coli* strains used in this study.

Strain	Relevant genotype [a]	Source or Reference
CC4711	*att*Tn7<>(*parS aph*) (at 84.2 min)	(Li et al., 2002)
CC4713	*parS aph* (at 33.8 min)	(Li et al., 2002)
BTH101	*cya*-99 *araD*139 *galE*15 *galK*16 *rpsL*1 *hsdR*2 *mcrA*1 *mcrB*1	Karimova & Ladant
DY329	*rph*1 IN(*rrnD-rrnE*) Δ(*argF-lac*)U169 *nadA*::Tn10 *gal*490 λ*cI*857 Δ(*cro-bioA*)	(Yu et al., 2000)
FB1*	DY329, *mreB*<>*aph*	(Bendezu and de Boer, 2008)
FB10*	PB103, *mreC*<>*aph*	(Bendezu and de Boer, 2008)
FB11*	PB103, *mreD*<>*aph*	(Bendezu and de Boer, 2008)
FB12*	PB103, *mreBCD*<>*aph*	(Bendezu and de Boer, 2008)
FB14*	PB103, *mreCD*<>*aph*	(Bendezu and de Boer, 2008)
FB30*	TB28, *mreBCD*<>*aph*	(Bendezu and de Boer, 2008)
FB38*	TB28, *mrdAB*<>*aph*	(Bendezu and de Boer, 2008)
FB54*	TB28, *rodZ::*EzTnkan (=*rod*2352)	This work
FB57	TB10, *yhdE*<>*cat*	This work
FB58*	TB10, *rodZ*<>*aph*	This work
FB59	TB10, *rodZ*155<>*aph*	This work
FB60*	TB28, *rodZ*<>*aph*	This work
FB61	TB28, *rodZ*155<>*aph*	This work
FB62*	TB10, *ispG*<>*aph*	This work
FB66	TB28, *yhdE*<>*cat*	This work
FB72	DY329, *mreB'-rfp-'mreB*	This work
FB74	DY329, *mreB'-rfp'-mreB yhdE*<>*cat*	This work
FB76	TB28, *mreB'-rfp-'mreB yhdE*<>*cat*	This work
FB80*	TB10, P_{rodZ}<>(*aph araC* P_{BAD})	This work
FB81*	TB28, P_{rodZ}<>(*aph araC* P_{BAD})	This work
FB83	TB28, *mreB'-rfp-'mreB yhdE*<>*frt*	This work
FB84*	FB76, P_{rodZ}<>(*aph araC* P_{BAD})	This work
FB85*	FB76, *rodZ*<>*aph*	This work
FB86	TB28, *parS aph* (at 33.8 min)	This work
FB87*	TB28, P_{rodZ}<>(*frt araC* P_{BAD})	This work
FB88*	FB87, *att*Tn7<>(*parS aph*) (at 84.2 min)	This work

FB89*	FB87, *parS aph* (at 33.8 min)	This work
FB90*	FB83, *mrdAB<>aph*	This work
FB91*	TB28, *ispG<>aph*	This work
FB93*	DY329, *mreB'-rfp-'mreB mreCD<>aph yhdE<>cat*	This work
FB95*	TB28, *mreB'-rfp-'mreB mreCD<>aph yhdE<>cat*	This work
FB101*	FB83, *rodZ<>aph*	This work
MG1655	*ilvG rfb*50 *rph*1	(Guyer et al., 1981)
Rod2352*	TB28, *rodZ::*EzTnkan (=*rod*2352)	This work
PB103	*dadR trpE trpA tna*	(de Boer et al., 1988)
TB10	MG1655, *nadA*::Tn10 λ*cI*857 Δ(*cro-bioA*)	(Johnson et al., 2004)
TB28	MG1655, *lacIZYA<>frt*	(Bernhardt and de Boer, 2003)
TB99	TB28, *att*Tn7<>(*parS aph*) (at 84.2 min)	This work

<> denotes DNA replacement by λ red recombineering, and *frt* a scar sequence remaining after eviction of an antibiotic resistance cassette with FLP recombinase (Datsenko and Wanner, 2000; Yu et al., 2000). Note that strains marked with * required an appropriate plasmid, phage, inducer and/or medium for survival.

Table S3. *E.coli* plasmids and phages used in this study.

Construct	Relevant genotype [a]	ori	Source or Reference
Plasmids:			
pBAD33	*cat araC*	pACYC	(Guzman et al., 1995)
pCH311	*bla lacI*^{q} P_{lac}::*zipA-rfp*	ColE1	This work
pCH356	*bla lacI*^{q} P_{lac}::*mreB'-t18-'mreB*	ColE1	This work
pCH358	*aph* P_{lac}::*t25-rodZ*	pACYC	This work
pCH363	*bla lacI*^{q} P_{lac}::*lacZ'-t18*	ColE1	This work
pCH364	*bla lacI*^{q} P_{lac}::*t18-'lacZ*	ColE1	This work
pCH371	*bla lacI*^{q} P_{lac}::*t18-rodZ*	ColE1	This work
pCH375	*aph* P_{lac}::*mreB'-t25-'mreB*	pACYC	This work
pCH378	*aph* P_{lac}::*t25-mreC*	pACYC	This work
pCH379	*aph* P_{lac}::*t25-pbpA* (*mrdA*)	pACYC	This work
pCH382	*bla lacI*^{q} P_{lac}::*t18-mreC*	ColE1	This work
pCH383	*bla lacI*^{q} P_{lac}::*t18-pbpA* (*mrdA*)	ColE1	This work
pCH384	*aph* P_{lac}::*t25-mreD*	pACYC	This work
pCH385	*aph* P_{lac}::*t25-rodA* (*mrdB*)	pACYC	This work
pCH386	*bla lacI*^{q} P_{lac}::*t18-mreD*	ColE1	This work
pCH387	*bla lacI*^{q} P_{lac}::*t18-rodA* (*mrdB*)	ColE1	This work
pCH393	*bla lacI*^{q} P_{lac}::*t18-rodZ*(1-84)-*malF*(1-39)-*rfp*	ColE1	This work
pCH406	*bla lacI*^{q} P_{lac}::*t18-rodZ*(1-84)-*malF*(1-14) -*rodZ*(111-337)	ColE1	This work
pCH414	*bla lacI*^{q} P_{lac}::*t18-rodZ*(83-337)	ColE1	This work
pCX16	*aadA sdiA*	pSC101	(Wang et al., 1991)
pDR3	*bla lacI*^{q} P_{lac}::*ftsZ*	ColE1	(Bernhardt and de Boer, 2005)
pFB105	*bla lacI*^{q} P_{T7}::*t-mreB*(2-347)-*h*	ColE1	This work
pFB174	*cat araC* P_{BAD}::*mreBCD*	pACYC	(Bendezu and de Boer, 2008)
pFB184	*bla lacI*^{q} P_{lac}::*sdiA*::*lacZ*	F	This work
pFB206	*cat araC* P_{BAD}::*mreCD*	pACYC	This work
pFB214	*bla lacI*^{q} P_{tac}::*mreB*	ColE1	This work
pFB216	*cat lacI*^{q} P_{tac}::*mreB*	pACYC	This work
pFB234	*bla lacI*^{q} P_{lac}::*ispG*	ColE1	This work
pFB235	*bla lacI*^{q} P_{lac}::*rodZ*::*ispG*	ColE1	This work

pFB237	*bla lacI*^{q} P_{lac}::*gfp-t-rodZ*	ColE1	This work
pFB254	*bla lacI*^{q} P_{T7}::*h-sumo-rodZ*(1-319)	ColE1	This work
pFB259	*bla lacI*^{q} P_{lac}::*mreB'-linker-'mreB*	ColE1	This work
pFB262	*bla lacI*^{q} P_{lac}::*mreB'-rfp-'mreB*	ColE1	This work
pFB273	*att*HK022 *bla lacI*^{q} P_{lac}::*gfp-t-rodZ*	R6K	This work
pFB274	*att*HK022 *bla lacI*^{q} P_{lac}::*gfp-parB*(31-333)	R6K	This work
pFB285	*att*HK022 *bla lacI*^{q} P_{lac}::*gfp-t-rodZ*(1-111)	R6K	This work
pFB289	*att*HK022 *bla lacI*^{q} P_{lac}::*gfp-t-rodZ*(1-111) *-malF*(17-39)*-rfp*	R6K	This work
pFB290	*bla lacI*^{q} P_{lac}::*rodZ*	ColE1	This work
pFB291	*bla lacI*^{q} P_{tac}::*rodZ*	ColE1	This work
pFB293	*att*HK022 *bla lacI*^{q} P_{lac}::*gfp-t-malF*(2-14*)-rodZ*(111-337)	R6K	This work
pFB299	*bla lacI*^{q} P_{tac}::*mreB::rodZ*	ColE1	This work
pFB309	*aadA* P_{syn135}::*gfp-t-rodZ*	pSC101	This work
pFB310	*aadA* $P_{\lambda R}$:: *mreB'-rfp-'mreB*	pSC101	This work
pFB312	*att*HK022 *bla lacI*^{q} P_{lac}::*gfp-t-rodZ*(83-138) *-rfp*	R6K	This work
pFB319	*att*HK022 *bla lacI*^{q} P_{lac}::*gfp-t-rodZ*(1-84) *-malF*(1-39)*-rfp*	R6K	This work
pFB321	*att*HK022 *bla lacI*^{q} P_{lac}::*gfp-t-rodZ*(1-84) *-malF*(1-14)*-rodZ*(111-337)	R6K	This work
pJE80	*cat araC* P_{BAD}::*sfiA*	pACYC	(Johnson et al., 2002)
pJF118EH	*bla lacI*^{q} P_{tac}	ColE1	(Furste et al., 1986)
pKT25	*aph* P_{lac}::*t25-*	pACYC	(Karimova et al., 2001)
pKNT25	*aph* P_{lac}::*lacZ'-t25*	pACYC	(Karimova et al., 2005)
pMLB1113	*bla lacI*^{q} P_{lac}::*lacZ*	ColE1	(de Boer et al., 1989)
pTB59	*bla lacI*^{q} P_{lac}::*mrdA mrdB*	ColE1	(Bernhardt and de Boer, 2004)
pTB63	*tet ftsQ ftsA ftsZ*	pSC101	(Bernhardt and de Boer, 2004)
pTB97	*att*HK022 *bla lacI*^{q} P_{lac}::*gfp-t-zapA*	R6K	This work
pTB98	*att*HK022 *bla lacI*^{q} P_{lac}::*zipA-gfp*	R6K	This work
pTB145	*bla lacI*^{q} P_{T7}::*h-ulp*1(403-621)	ColE1	This work
pTB146	*bla lacI*^{q} P_{T7}::*h-sumo*	ColE1	This work
pTB183	*att*HK022 *bla lacI*^{q} P_{lac}::*gfp-t-zapA*	R6K	This work

pTB222	*att*HK022 *bla lacI*^{q} P_{lac}::*zipA-gfp*	R6K	This work
pUT18	*bla* P_{lac}::*lacZ'-t18*	ColE1	(Karimova et al., 2001)
pUT18C	*bla* P_{lac}::*t18-*	ColE1	(Karimova et al., 2001)
pYT22	*att*HK022 *bla lacI*^{q} P_{lac}::*gfp-t-rodZ*(1-138) *-rfp*	R6K	This work
pYT27	*att*HK022 *bla lacI*^{q} P_{lac}::*gfp-t-rodZ*(83-337)	R6K	This work
Phages:			
λFB234	*imm*^{21} *bla lacI*^{q} P_{lac}::*ispG*	λ	This work
λFB237	*imm*^{21} *bla lacI*^{q} P_{lac}::*gfp-t-rodZ*	λ	This work

[a]Genotypes indicate when constructs encode in-frame Gfpmut2 (*gfp*), mCherry (*rfp*), T7.tag, (*t*), hexahistidine (*h*), yeast SUMO domain (*sumo*), CyaA T18-domain (*t18*), or CyaA T25-domain (*t25*) sequences.

Figure S1

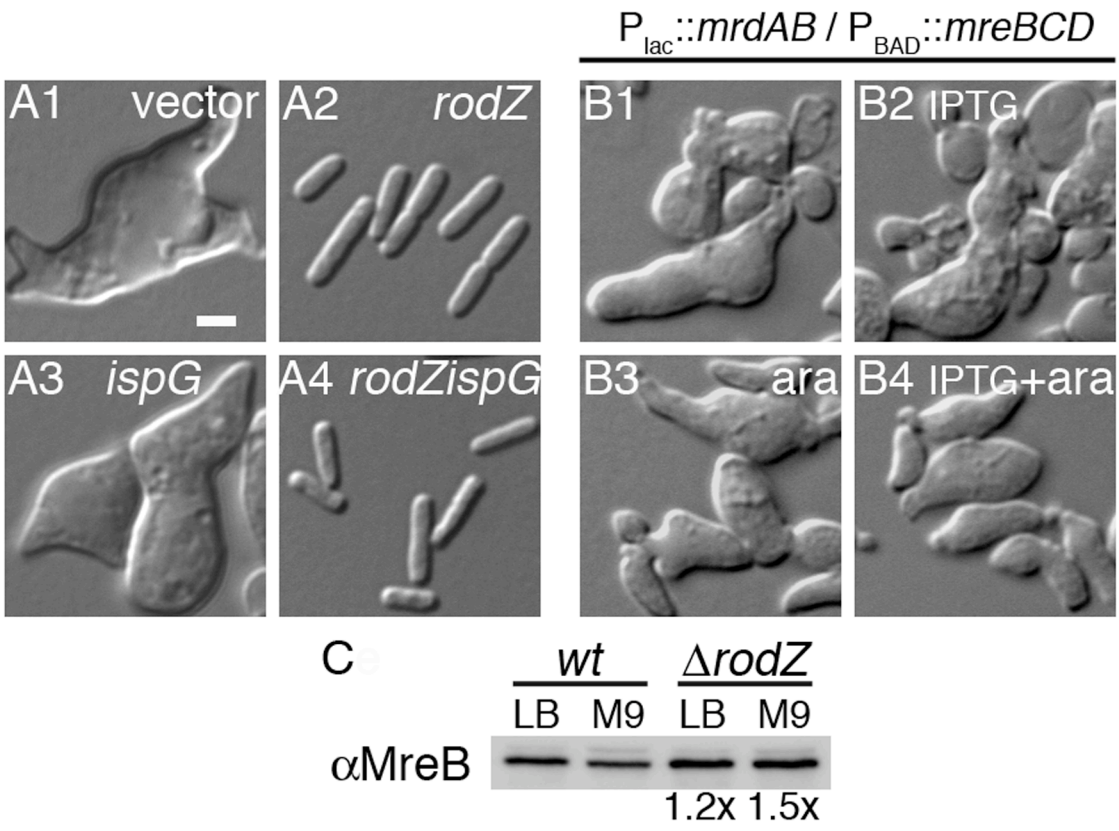
P lac ::mrdAB / P BAD ::mreBCD
A1 vector
A2 rodZ
B1
B2 IPTG
A3 ispG
A4 rodZispG
B3 ara
B4 IPTG+ara
C
wt
ΔrodZ
LB M9 LB M9
αMreB
1.2x 1.5x

Figure S2

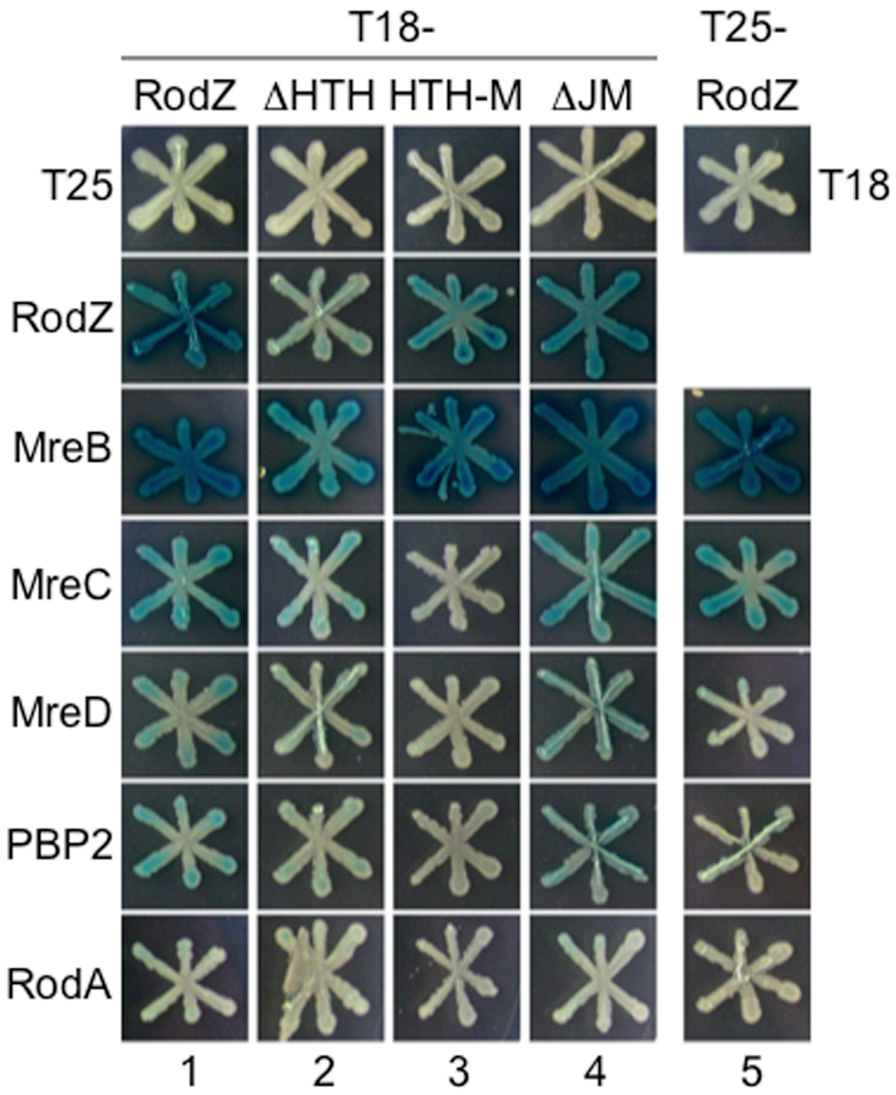
T18-
T25-
RodZ
ΔHTH
HTH-M
ΔJM
RodZ
T25
T18
RodZ
MreB
MreC
MreD
PBP2
RodA
1
2
3
4
5

Figure S3

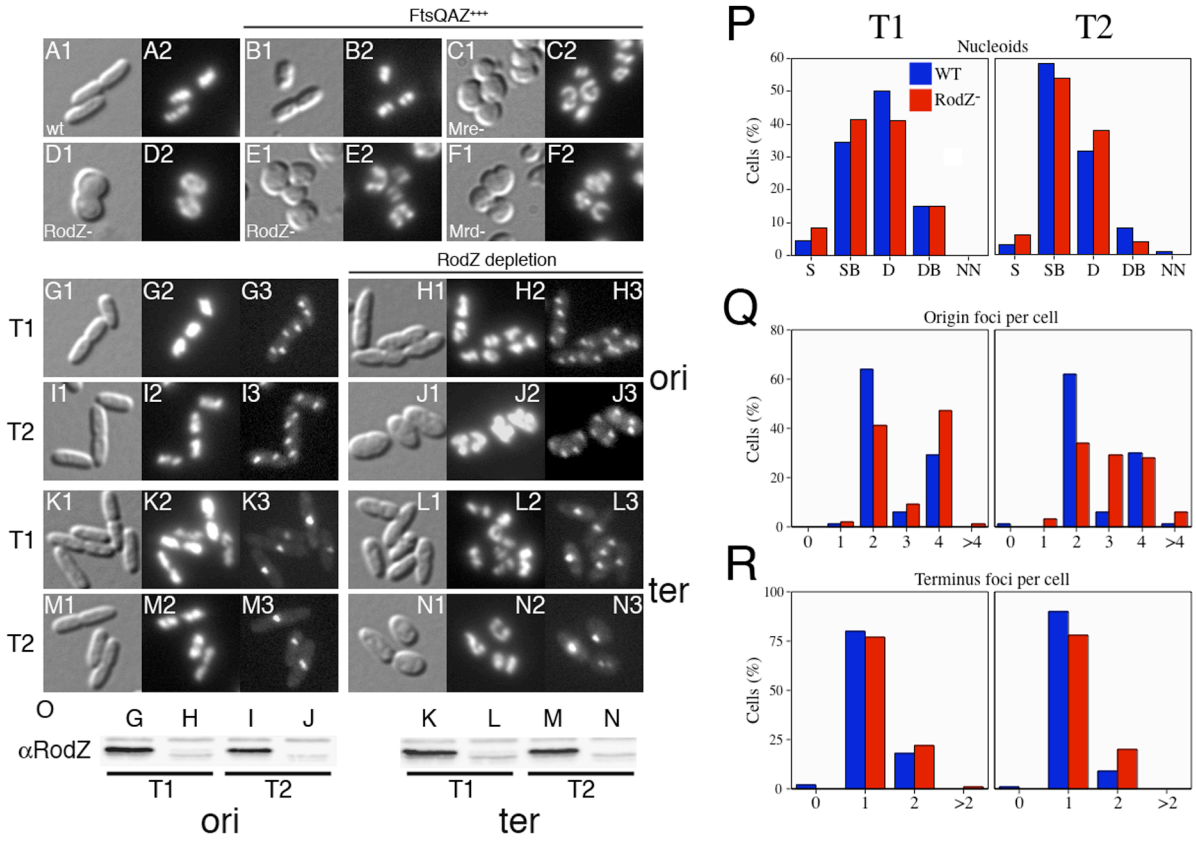
FtsQAZ+++
A1
A2
wt
B1
B2
C1
C2
Mre-
D1
D2
RodZ-
E1
E2
RodZ-
F1
F2
Mrd-
RodZ depletion
G1
G2
G3
H1
H2
H3
T1
ori
I1
I2
I3
J1
J2
J3
T2
K1
K2
K3
L1
L2
L3
T1
ter
M1
M2
M3
N1
N2
N3
T2
O
G
H
I
J
K
L
M
N
αRodZ
T1
T2
T1
T2
ori
ter
P
T1
T2
Nucleoids
WT
RodZ-
Cells (%)
S
SB
D
DB
NN
Q
Origin foci per cell
Cells (%)
R
Terminus foci per cell
Cells (%)

Figure S4

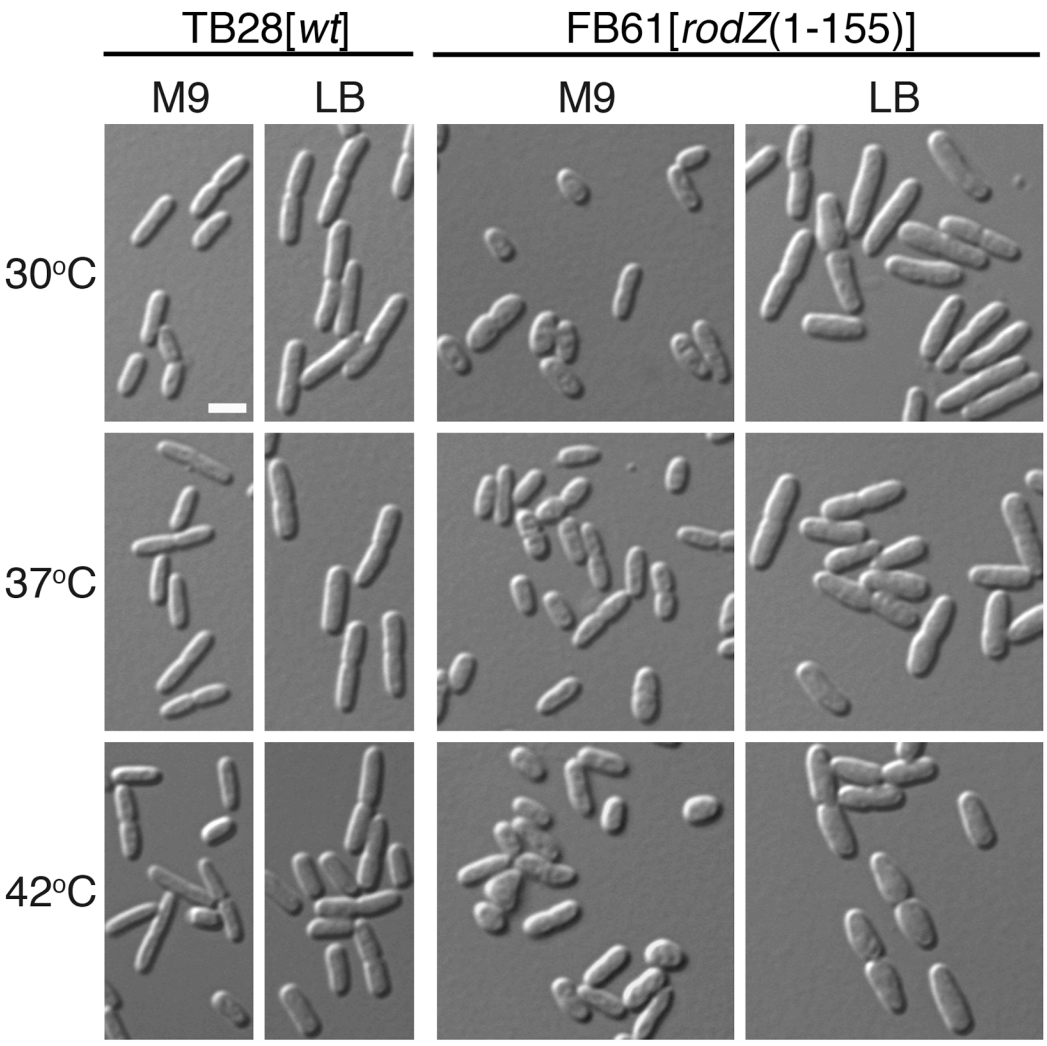

Medium	Temp. °C	FB61:TB28	
		length	width
M9-mal	30	0.66	1.22
	37	0.82	1.17
	42	0.94	1.45
LB	30	1.13	1.14
	37	0.99	1.25
	42	1.05	1.29

Figure S5

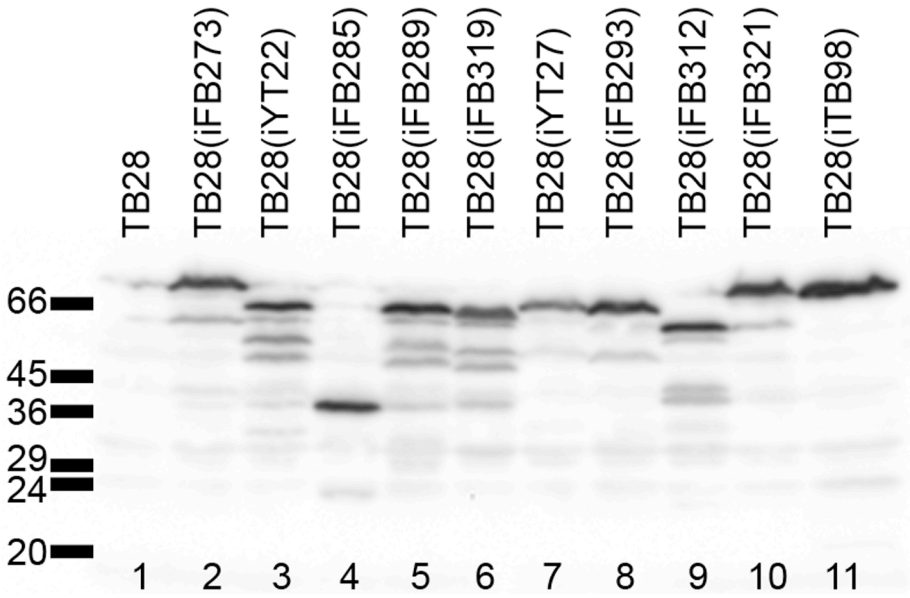
TB28
TB28(iFB273)
TB28(iYT22)
TB28(iFB285)
TB28(iFB289)
TB28(iFB319)
TB28(iYT27)
TB28(iFB293)
TB28(iFB312)
TB28(iFB321)
TB28(iTB98)
66
45
36
29
24
20
1
2
3
4
5
6
7
8
9
10
11

LEGENDS TO SUPPLEMENTAL FIGURES

Figure S1. Complementation of Δ*rodZ* by *rodZ* plasmids, and MreB levels in Δ*rodZ* cells.

A, DIC images of chemically fixed cells of strain FB60 [Δ*rodZ*] harboring pMLB1113 [vector] (1), pFB290 [P_{lac}::*rodZ*] (2), pFB234 [P_{lac}::*ispG*] (3), or pFB235 [P_{lac}::*rodZ ispG*] (4). Cells were grown overnight at 30°C in M9-mal with 100 μM IPTG to OD_{600}=0.02 (1, 3) or 1.10 (2, 4). Cells were then diluted to OD_{600}=0.01 (1, 3) or 0.05 (2, 4) into LB with 100 μM IPTG, and growth was continued at 30°C to OD_{600}=0.03 (1, 3) or 0.60 (2, 4).

B, DIC images of fixed cells of strain FB60/pTB63/pTB59/pFB174 [Δ*rodZ* /P_{QAZ}::*ftsQAZ* /P_{lac}::*mrdAB* /P_{BAD}::*mreBCD*]. An overnight culture was diluted 1:400 into LB lacking inducers (1), or supplemented with 50 μM IPTG (2), 0.5% arabinose (3), or both 50 μM IPTG and 0.5% arabinose (4). Growth at 30°C was continued to OD_{600}=0.6.

C, Western showing that MreB is not lacking in Δ*rodZ* cells. Whole-cell extracts were prepared from cells of strains TB28 [wt] and FB60 [Δ*rodZ*] that had grown at 37°C in LB or M9-mal as indicated. Cells were harvested at OD_{600}=0.6, except for FB60 in M9-mal (second lane), which were harvested at OD_{600}=0.2. Each lane received 20 μg total protein and MreB was detected with anti-MreB antiserum. MreB levels in FB60, relative to the *wt* controls, are given under the relevant lanes.

Figure S2. BACTH analyses.

Plasmid pairs encoding the indicated T18- and T25- fusions were co-transformed into BTH101 [*cya*-99], and individual colonies were patched on M9-glucose agar containing 50 μg/ml Amp, 25 μg/ml Kan, 40 μg/ml X-Gal, and 250 μMIPTG. Plates were incubated at 30°C and inspected after 24, 30, and 36 hr. The figure shows results at 30 h. Patches were rearranged for clarity of the figure. The panels in each row were taken from a single image of a single plate, each plate was from the same batch, and all plates were processed and imaged concurrently and under identical conditions. Each row of assays was repeated at least twice, yielding identical results.

Figure S3. RodZ is not required for chromosome segregation.

A-F, DAPI staining of nucleoids in TB28 [wt] (A, B), FB30 [Δ*mreBCD*] (C) , FB60 [Δ*rodZ*] (D, E), and FB38 [Δ*mrdAB*] (F) cells. Cells were either plasmid-free (A, D), or harbored pTB63 [*ftsQAZ*] (B, C, E, F) to suppress the division defect associated with loss of cell shape. Cells were grown at 30°C in M9-mal to OD_{600}=0.3, chemically fixed, treated with DAPI (0.25 μg/ml), and imaged with DIC (1) and DAPI fluorescence (2) optics. Inspection of 200 Δ*rodZ* cells revealed no nucleoid-free cells (< 0.5%).

G-R, Segregation of origin and terminus regions in WT and RodZ-depleted cells.

The locations of origin or terminus regions of the chromosome were monitored by determining the location of a GFP-tagged version of P1 ParB in strains that carry its cognate *parS* site integrated near *oriC* (G-J) or *dif* (K-N). Strains used were TB99(iFB274) [*oriC-parS* (P_{lac}::*gfp-Δ30parB*)] (G and I), FB88(iFB274) [*oriC-parS* P_{BAD}::*rodZ* (P_{lac}::*gfp-Δ30parB*)] (H and J), FB86(iFB274) [*dif-parS* (P_{lac}::*gfp-Δ30parB*)] (K and M) and FB89(iFB274) [*dif-parS* P_{BAD}::*rodZ* (P_{lac}::*gfp-Δ30parB*)] (L and N). Cells were grown overnight at 30°C in M9-mal supplemented with 0.5% arabinose. They were then diluted to OD_{600}=0.01 into M9-mal with 100 μM IPTG, but lacking arabinose (to deplete RodZ in FB88 and FB99), and growth was continued. At OD_{600}=0.1 (T1) and 0.4 (T2) aliquots were taken for cell imaging (G-N), and Western analyses (O). For imaging (G-N), cell were fixed, treated with DAPI to stain entire nucleoid(s), and observed with DIC (1), DAPI fluorescence (2), and GFP fluorescence (3) optics.

For the Western analyses in panel O, each lane received 10 μg of total protein, and RodZ was detected with anti-RodZ antserum. Lane designations correspond to the image panels described above. Note that RodZ had been effectively depleted in both FB88(iFB274) and FB89(iFB274) depletion strains at both the T1 (H, L) and T2 (J, N) time points even though cells were clearly still rod-shaped, especially at T1 (H and L).

Panels P-R show measurements of cellular parameters performed on 100 cells from each of the RodZ-depletion (red bars) and corresponding WT (blue bars) cultures described above, at both T1 (left histograms) and T2 (right histograms). Panel P summarizes the appearance of whole nucleoids as inferred from DAPI images. Shown are the percentages of cells with (from left to right): a single nucleoid mass (S); a single bilobed nucleoid mass (SB); two separated nucleoid masses (double, D); two separate bilobed nucleoid masses (DB); and no nucleoid (NN). Panel Q shows the percentages of cells with (from left to right) 0, 1, 2, 3, 4, or >4 origin foci, and panel R the percentages of cells with (from left to right) 0, 1, 2, or >2 terminus foci. Note that there is little difference in overall nucleoid appearance, or in the cellular number of origin and termini foci, between WT and RodZ-depleted cells.

Figure S4. Only mild shape defects in cells lacking the periplasmic domain of RodZ.

Overnight cultures of strains TB28 [wt] and FB61 [*rodZ*(1-155*)*] were diluted to OD_{600}=0.05 into LB or M9-mal and growth was continued at 30^{o}C, 37^{o}C, or 42^{o}C to OD_{600}=0.5. Cells were fixed and imaged by DIC microscopy. Average length and width from 50 cells of each culture was determined. Panel A shows examples of cells from each culture, and panel B gives the ratios of average lenghts and widths of FB61 cells to TB28 cells for each of the six growth conditions.

Figure S5. Immunoblot of GFP-RodZ domain deletion/substitution derivatives.

Strains used are identified above each lane. Cells were grown as described in the legend to Figure 6 in the presence of 50 μM (lane 11) or 250 μM (all other lanes) IPTG to OD_{600}=0.4. An equivalent amount of whole-cell lysate was loaded in each lane, and GFP-RodZ variants were detected with Goat α-GFP antibodies (Rockland). Strains TB28 [wt] (lane 1) and TB28(iTB98) [wt(P_{lac}::*zipA-gfp*)] (lane 11) served as negative and positive controls, respectively. Note that native RodZ (36.2 kD) migrates abberantly in SDS-PAGE gels as a protein that is 15-20 kD larger. Such slow migration is also apparent with each GFP-RodZ variant that still contains its native periplasmic domain (lanes 2, 7, 8, and 10), but not in those in which this domain has been removed (lane 4) or substituted with RFP (3, 5, 6, and 9). We infer that it is the periplasmic domain of RodZ that causes its slow migration in SDS-PAGE gels.

A genetic screen for cell shape mutants, and isolation of *rodZ::*EzTnkan.

In *E.coli*, the five known cell shape maintenance proteins MreBCD and MrdAB are all conditionally essential for growth (Bendezu and de Boer, 2008). Cells lacking any of these proteins propagate stably as small spheres at low mass doubling rates, but form giant non-dividing spheroids at higher ones. An extra supply of the FtsZ division protein, however, suppresses lethality by allowing the shape mutants to propagate as small dividing spheres at higher rates as well.

We made use of this latter property in a screen for additional cell shape factors by selecting for mutants that: i) required additional FtsZ for survival or good growth on rich medium, and ii) showed a cell shape defect. The screen was similar to synthetic lethality screens we developed before (Bernhardt and de Boer, 2004; Bernhardt and de Boer, 2005), and relied on enhanced retention of an unstable F plasmid derivative (pFB184 [*bla lacI*^{q} P_{lac}::*sdiA*::*lacZ*]) encoding both SdiA and LacZ under control of the *lac* regulatory region. SdiA stimulates transcription of the *ftsQAZ* genes (Wang et al., 1991), and cells harboring pFB184 produce extra FtsZ in the presence of IPTG. The plasmid was introduced in TB28 [Δ*lacIZYA*], which lacks the chromosomal *lac* operon, and TB28/pFB184 cells were subjected to random mutagenesis with EZTnkan-2 (Epicentre).

For mutagenesis, TB28/pFB184 cells were grown overnight at 30^{o}C in LB-Amp with 0.1% glucose, diluted 1:400 into LB-Amp with 50 μM IPTG, grown at 37^{o}C to OD_{600}=0.46, and subjected to electroporation with EZTnKan-2 transposome as described (Bernhardt and de Boer, 2004). Electroporated cells were resuspended in LB-Amp with 50 μM IPTG and incubated statically at room temperature for 10 min. followed by shaking at 30^{o}C for 90 min. They were then plated on M9-maltose agar containing Kan, Amp and 100 μM IPTG at a density of about 5.5x!0^4 Kan-resistant c.f.u./plate, and incubated for 44 hrs at room temperature. The lawns of four such plates were resuspended in 3.5 ml LB total, 2.5 ml of 40% glycerol was added, and the library was stored in aliquots at -80^{o}C.

For *rod* screens, an aliquot of the library was diluted in LB and plated at a density of 100-200 c.f.u./plate on LB-IX-agar, containing 100 μM IPTG and 40μg/ml Xgal, but no antibiotics. After incubation at 30^{o}C for 48 hr, the vast majority of transposon mutants formed white or sectored-blue colonies, reflecting rapid loss of the plasmid. Some formed solid-blue colonies, however, suggesting that retention of the plasmid provided a selective advantage. The latter were purified on LB-Xgal with either 100 μM IPTG or 0.1% glucose, to be tested for SdiA-dependent growth and cell morphology. Out of a total of 3.3x10^5 colonies screened, 76 were

retained for further analysis. Transposon insertion sites were determined as described (Bernhardt and de Boer, 2004; O'Toole and Kolter, 1998).

As expected, the screen yielded insertions in genes/operons known to affect cell division and/or cell shape, including *zipA*, *ftsEX*, *ddlB*, *mraZ*, *min*, *mre* and *mrd* (Bendezu and de Boer, 2008; de Boer et al., 1990; Flardh et al., 1998; Geissler et al., 2003; Mengin-Lecreulx et al., 1998; Reddy, 2007; Vinella et al., 1993), as well as in uncharacterized genes.

Mutant Rod2352/pFB184 [*rodZ::*EzTnkan/ P_{lac}::*sdiA*::*lacZ*] formed mostly solid blue colonies on LB-IX, as well as some small white ones, suggesting that occasional loss of the plasmid was detrimental to growth. Because it propagated as spheroids and EZTnkan-2 had inserted in a gene of unknown function, it was chosen for further study.

Depletion of RodZ does not greatly affect chromosome segregation.

The MreB cytoskeleton has been implicated in chromosome segregation (Defeu Soufo and Graumann, 2005; Gitai et al., 2005; Kruse et al., 2006; Kruse et al., 2003; Soufo and Graumann, 2003). Given its putative DNA-binding domain RodZ would be an attractive candidate for mediating MreB-directed nucleoid dynamics. Inspection of DAPI-treated FB60 [ΔrodZ] cells failed to reveal DNA-less cells (0/200) or any other gross nucleoid segregation defects Fig.S3D and E). However, nucleoid staining patterns in spherical cells are a bit difficult to interpret with confidence. Moreover, even if RodZ were not required for bulk segregation, it might still be more specifically involved in the directed poleward movements of newly replicated origin regions, which are proposed to depend on the MreB cytoskeleton. To test this, we examined RodZ-depletion strains in which the location of the *oriC* or *ter* regions of the chromosome can be visualized by the P1 parS/GFP-Δ30ParB system (Li et al., 2002). We slightly modified this system in that GFP-Δ30ParB was encoded on the chromosome rather than on a multicopy plasmid, affording better control over its production. Thus, TB99(iFB274) and the isogenic RodZ-depletion strain FB88(iFB274) harbor a P_{lac}::*gfp-Δ30parB* cassette at *att*HK022 and a single copy of *parS* at 84.2' near *oriC*. In addition, FB88(iFB274) contains a chromosomal P_{BAD}::*rodZ* allele, allowing facile depletion of RodZ. Cells were inoculated in M9-mal with IPTG (100μM), but lacking arabinose, and then monitored for RodZ levels, cell morphology, and nucleoid and *ori*C separation after 3.3 (T1) and 5.3 (T2) mass doublings. RodZ was barely detectible in FB88(iFB274) cells at either time point, but, while cells had begun to round up at T2, most still had a distinct rod-shape at T1 (FigS3). Analyses of the nucleoids and origin foci in these cells failed to reveal significant differences with that of the wt control (Fig.S3). Moreover, we did not detect any obvious effects of RodZ-depletion on localization of the *ter* region, using a

similar set of strains that contain a single *parS* site near ter, at 33.8' (Fig.S3). These results indicate that a lack of RodZ has little if any direct effect on chromosome dynamics.

The periplasmic (P) domain of RodZ is dispensible for cell growth, shape maintenance and RodZ localization.

In a genomic analysis of essential genes by genetic footprinting, *rodZ* (*yfgA*) was classified as a non-essential gene because transposon insertions in codons 156, 182, 216 and 280 (indicated in Fig.1A) were apparently well-tolerated by cells growing in rich medium (Gerdes et al., 2003). This suggested that the C-terminal portion of RodZ might be dispensible for good growth and cell shape maintenance. To test this, we first engineered a strain bearing a translation stop after codon 155 of chromosomal *rodZ* (Fig.1A). Notably, FB61[*rodZ*$^{1\text{-}155}$] cells grew well and were still rod-shaped in both minimal and rich growth medium, though they were upto 45% wider on average than cells of the *wt* parent TB28 (Table 1, Fig.S4).

The implication that the periplasmic domain is largely dispensible for the roles of RodZ in proper growth and cell shape maintenance was further verified in a more comprehensive domain analysis effort. To this end, we created a set of derivatives of the integrative CRIM construct pFB273 [P_{lac}::*gfp-rodZ*], encoding mutant variants of GFP-RodZ in which one or more of the HTH, basic JM, TM, and P domains is missing or replaced with heterologous peptides. TB28 [wt] and FB60 [Δ*rodZ*] strains bearing such an integrated construct were then grown in M9-mal in the presence of IPTG and examined for growth rate, cell morphology, and localization of the RodZ variant (Fig.6, Table 3). Western analyses indicated that none of the variants were subject to excessive degradation (Fig.S5).

Production of a GFP-RodZ$^{1\text{-}138}$-RFP fusion, in which almost the complete P domain is replaced with mCherry RFP, was indeed sufficient to restore both rod-shape and doubling times of FB60(iYT22) cells (Fig.6B, Table 3). Moreover, the fusion still localized in a spiral-like fashion in the resulting rods (Fig.6B1), and the same localization pattern was evident in *wt* cells of TB28(iYT22) (Fig.6B2).

In contrast, a GFP-MalF$^{2\text{-}14}$-RodZ$^{111\text{-}337}$ fusion in which the entire cytoplasmic part of RodZ (HTH+JM) is replaced with a cytoplasmic portion of the MalF protein, neither restored rod-shape to FB60(iFB293) cells, nor alleviated their slow growth rate. Moreover, the fusion distributed

rather evenly along the membrane of both Δ*rodZ* speroids and *wt* cells, suggesting that the P domain contributes little to the typical spiral-like localization of RodZ (Fig.6G, Table 3).

Thus, while the cytoplasmic part of RodZ ($RodZ^{1-111}$) is required for its spiral localization and for normal cellular viability and rod-shape, the periplasmic part of RodZ is dispensible for these functions, although it may help to fine-tune the precise dimensions of cells.

Role of the trans-membrane (TM) domain of RodZ.

A soluble GFP-$RodZ^{1-111}$ fusion failed to correct the growth and shape defects of Δ*rodZ* FB60(iFB285) cells, and distributed throughout the cytoplasm of Δ*rodZ* spheroids and *wt* rods (Fig.6C, Table 3). This result indicated that, in addition to its cytoplasmic portion, the TM domain of RodZ was also critical to its functions.

To assess if RodZ specifically requires its native TM, we studied GFP-$RodZ^{1-111}$-$MalF^{17-39}$-RFP, a fusion that is identical to the functional GFP-$RodZ^{1-138}$-RFP fusion described above, except that RodZ's TM has been replaced with the first TM helix (TM1) of the MalF protein (Guzman et al., 1997). Interestingly, this fusion allowed FB60(iFB289) cells to grow at a near normal rate, and it localized in spiral-like patterns in both Δ*rodZ* and *wt* cells (Fig6D, Table 3). The fusion also restored rod-shape to Δ*rodZ* cells to an appreciable extent, but was clearly less effective in doing so than GFP-$RodZ^{1-138}$-RFP or full-length GFP-RodZ. Thus, about half the population of FB60(iFB289) cells were rods of variable widths but the rest had an ovoid, spherical, or more irregular appearance (Table 3).

We infer that there is a strict requirement for the cytoplasmic portion of RodZ ($RodZ^{1-111}$) to be tethered to the membrane in order for it to support normal cell growth and shape, as well as to localize in its normal spiral-like pattern. In addition, while there is no strict requirement for $RodZ^{1-111}$ to be tethered via its native TM in order to promote rod shape per se, substitution of the TM clearly reduced its efficacy in doing so.

The helix-turn-helix (HTH) domain of RodZ is a major localization determinant, but not strictly essential for rod-shape and good growth.

Importantly, a fusion lacking the complete HTH domain (GFP-$RodZ^{83-337}$) was still capable of restoring good growth to Δ*rodZ* FB60(iYT27) cells (Table 3). Moreover, the fusion restored rod-shape to a majority of cells (Fig.6F), though many rods appeared wider than normal and the rest of the population (~ 25%) still showed irregularities such as uneven width, branching, and/or a

spheroidal shape (Table 3). However, the most striking difference between this and other functional fusions was its distribution. Thus, whereas GFP-RodZ and other membrane-associated HTH-containing fusions showed a clear spiral-like distribution in virtually all cells, GFP-RodZ$^{83-337}$ distributed far more evenly along the membrane in both corrected Δ*rodZ* rods and *wt* cells (Fig.6F). The distribution was not completely homogenous, however, as some small spots of relatively high signal could still be detected along the periphery of cells (Fig.6F3,4), suggesting that some fraction of the fusion molecules still accumulated in a more organized fashion.

These result showed that the HTH domain of RodZ is not strictly required for good growth or a rod shape of cells per se, but that it does contribute significantly to the typically sharp spiral-like distribution of the protein. Confirmation of the latter came from studying GFP-RodZ$^{1-84}$-MalF$^{1-39}$-RFP, a membrane-tethered version of just the HTH domain. Whereas this fusion failed to correct the growth and shape defects of Δ*rodZ* cells, it localized in distinct foci along the periphery of FB60(iFB319) spheres, and in a spiral-like fashion in *wt* rods (Fig.6E, Table 3). In contrast, a soluble GFP-RodZ$^{1-84}$ fusion behaved like GFP-RodZ$^{1-111}$, and dispersed throughout the cytoplasm of both Δ*rodZ* spheres and *wt* rods (not shown). We conclude that, as long as it is membrane-tethered, the HTH domain of RodZ is a dominant determinant of the normal spiral-like distribution of the protein.

The basic juxta-membrane (JM) domain is critical but not sufficient for RodZ function.

The results obtained above pointed to a critical role for the JM domain in the maintenance of both good growth and rod shape by RodZ. This was supported by the properties of a mutant version of GFP-RodZ in which this domain is replaced with a juxta-membrane portion of MalF (also basic, +3). Even though GFP-RodZ$^{1-84}$-MalF$^{1-16}$-RodZ$^{111-337}$ localized in a spiral-like fashion in *wt* cells and in peripheral foci in FB60(iFB321) spheroids, it was incapable of correcting the growth and shape defects of the latter (Fig.6I, Table 3).

Finally, to test the distinct possibility that the JM and TM domains might in fact be sufficient for RodZ function, we next studied a GFP-RodZ$^{83-138}$-RFP fusion containing just these domains. Production of this fusion in FB60(iFB312) cells, however, failed to suppress their growth and shape defects, and the fusion distributed evenly along the membrane of mutant or *wt* cells (Fig.6H, Table 3).

Thus, in summary, our domain analyses revealed that both normal growth rate and cell shape is strictly dependent on the presence of a membrane-anchored juxta-membrane domain of RodZ, and that, additionally, the JM-TM part of RodZ needs to either be preceded by its cytoplasmic HTH domain, or followed by its periplasmic domain.

Microscopy.

The cells in Fig.3E-I were imaged on a Nikon 90i microscope equipped with a 100X (1.45 numerical aperture) oil objective. Fluorescence imaging was done using an X-Cite 120 fluorescence illuminator (EXFO) and RFP-specific (532- to 587-nm excitation filter, 595-nm dichroic mirror, and 608- to 683-nm barrier filter) and/or GFP-specific (450- to 490-nm excitation filter, 495-nm dichroic mirror, and 500- to 550-nm barrier filter) filter sets. Optical sections were collected with a CoolSNAP HQ camera (Photometrics). As indicated, optical slices from either the top (F, G, H3,and I3) or middle (E, H4, and I4) of the cell are shown. All other imaging was performed on a Zeiss Axioplan-2 microscope as previously described (Johnson et al., 2002). Live cells were imaged on 1.2% agarose pads made with either 0.5% NaCl (for LB cultures) or M9 salts (for M9 cultures). When indicated, cells were chemically fixed as previously described (Bendezu and de Boer, 2008) and DAPI was added to fixed cells at a concentration of 0.25 μg/ml 2 minutes prior to imaging.

Protein purification and αMreB and αRodZ antibodies.

Anti-MreB antiserum was raised against T-MreB(2-347)-H, a 39.3 kDa fusion in which the starting residue of MreB has been substituted with the T7.tag (MASMTGGQQMGRGS), and the peptide $LE(H)_6$ has been appended to its C-terminus. Strain BL21(λDE3)/plysS/pFB105 was grown overnight in LB supplemented with Amp, Cam, and 0.1% glucose. Cells were diluted 150-fold in 2 liter of LB-Amp with 0.04% glucose and grown at 30°C to OD_{600}=0.5. IPTG was added to 840 μM, and growth was continued for 2 hrs. Cells were harvested by centrifugation, washed in 60 ml saline, resuspended in 20 ml NiB(70/50) [20 mM Tris.Cl, 70 mM NaCl, 50 mM imidazole, pH=8.0], and broken by freeze-thawing, and mild sonication (Lackner et al., 2003). The suspension was subjected to centrifugation at 5,800 x g for 15 min at 4°C. Virtually all the fusion protein was present in inclusion bodies in the pellet fraction. This fraction was washed once in 20 ml of NiB(70/50) containing 0.1 % Triton X-100, and twice in 10 ml of NiB(70/50) without detergent. The washed inclusion bodies were resuspended in 12 ml of 8M urea in NiB(70/50) by mild sonication, and solubilized by incubation at 65°C for 2 h. The cleared suspension was subjected to centrifugation at 16,000 x g for 15 min at 4°C, and the supernatant

was diluted two-fold by addition of 8M urea in NiB(70/50). Per run, a 2 ml aliquot was loaded on a 0.5 ml fast-flow chelating Sepharose column (Pharmacia) that had been charged with $NiCl_2$ and equilibrated with 6 M urea in NiB(70/50). The column was washed with 6 M urea in NiB(70/50), and bound protein was eluted in the same buffer, but containing 200 mM imidazole. Appropriate fractions were pooled, and dialyzed to 4 M urea in buffer A (20 mM Tris.Cl, 25 mM NaCl, 2 mM EDTA, pH=8.0). The dialysate was further fractionated on a MonoQ column, using a linear 25-500 mM NaCl gradient in buffer A containing 4 M urea. Purified T-MreB(2-347)-H was dialyzed to 2 M urea in buffer B (20 mM Tris.Cl, 100 mM NaCl, pH=8.0), and then to buffer B without urea. Once solubilized, virtually all of the protein remained soluble during the purification steps. The protein was used to immunize Rabbits, as well as to affinity-purify αMreB antibodies from immune serum, as described (Addinall and Lutkenhaus, 1996).

Antigen for raising anti-RodZ antiserum was obtained using SUMO fusion technology (Marblestone et al., 2006; Mossessova and Lima, 2000). Plasmid pFB254 [P_{T7}::*h-sumo-rodZ*(1-319)] encodes a UlpI-cleavable His_6-SUMO tag fused to the N-terminus of RodZ. The plasmid inadvertently harbored an AGA (R) to TGA (STOP) mutation in RodZ codon 320, such that the purified antigen lacked the C-terminal 18 residues of native RodZ. An overnight culture of strain Rosetta(λDE3)/plysSRARE/pFB254, grown in LB-Amp-Cam with 0.1% glucose, was diluted 1:50 into 1 liter of LB-Amp-Cam with 0.04% glucose and grown at 30°C to OD_{600}=0.75. IPTG was added to 840 μM, and growth was continued for 2.5 hrs to OD_{600}=1.42. Cells were harvested by centrifugation at 2,600 x g for 20 minutes at 4°C, washed once in 20 ml ice cold 0.9% NaCl, resuspended in 10 ml cell lysis (CL) buffer (50 mM NaH_2PO_4, 300 mM NaCl, 10 mM Imidazole, pH 8.0), flash frozen in dry ice-acetone, and stored at -80°C. Cells were broken as described above, and insoluble material was sedimented at 6,000 x g for 15 minutes at 4°C and resuspended in 10 ml CL buffer. Triton X-100 was added to 0.5%, and the suspension gently shaken overnight at 4°C. After another round of centrifugation (6,000 x g for 15 minutes at 4°C), the resulting supernatant was highly enriched in H-SUMO-RodZ protein. The pellet was washed once in 10 ml CL buffer with 0.5 % triton X-100 and the combined supernatants were loaded onto 2 x 0.5 ml columns of NiNTA-agarose (Qiagen) pre-equilibrated in CL buffer with 0.5% Triton X-100. The columns were washed with 4 ml column buffer (C buffer; 50 mM NaH_2PO_4, 300 mM NaCl, 0.05% Triton X-100, pH 8) containing 20 mM imidazole, followed by 1 ml C buffer containing 50 mM imidazole. The H-SUMO-RodZ(1-319) protein was then eluted with three 0.5 ml fractions of C buffer containing 100 mM imidazole, three 0.5 ml fractions of C buffer with 250 mM imidazole and 2 0.5 ml fractions of C buffer with 500 mM imidazole. Peak fractions were

collected and dialyzed extensively into UlpI protease buffer (P buffer; 50 mM Tris-Cl, 150 mM NaCl, 10% glycerol, 1mM DTT, 0.05 % Triton X-100, pH 8). H-UlpI protease was added to a final molar ratio of 1:500 and the mixture was incubated overnight on ice. The mixture was passed over a 0.5 ml NiNTA-agarose column equilibrated in P buffer without glycerol to capture the His-tagged protease and freed H-SUMO tag. The flowthrough, containing tag-less RodZ(1-319) protein, was dialyzed against 20 mM Tris-Cl(pH 8), 25 mM NaCl, 1 mM EDTA, 0.05% Triton X-100, and further fractionated by anion exchange chromatography on a Mono-Q column (Pharmacia) with a linear 25-1000 mM NaCl gradient in the same buffer. The majority of RodZ(1-319) eluted between 200 and 300 mM NaCl. Pooled fractions were stored at -80^{o}C, and aliquots were subsequently used to immunize rabbits.

***E. coli* plasmids and phages.**

The most relevant plasmids and phages used in this study are listed in Table S3.

Plasmids pMLB1115 and pRC7 (de Boer et al., 1989), pZC100 (Wang et al., 1991), pDR123 (Raskin and de Boer, 1997), pDB311 (Hale and de Boer, 1997), pUNI10 (Liu et al., 1998), pCP20, pKD3 and pKD13 (Datsenko and Wanner, 2000), pAH61 and pCAH63 (Haldimann and Wanner, 2001), pKT25, pUT18, and pUT18C (Karimova et al., 2001), pJE42 (Johnson et al., 2002), pALA2705 (Li et al., 2002), pCH151 and pTB29 (Bernhardt and de Boer, 2003), pTB6 (Bernhardt and de Boer, 2004), pCH260 and pDR144 (Bernhardt and de Boer, 2005), pDB366, pCH214, pCH233, pCH235, pCH244, pCH268, pFB124, pFB149, pFB174, and pTB188 (Bendezu and de Boer, 2008) were described previously. pET21 was obtained from Novagen, pTYB12 from New England Biolabs, and pBT3-N and pPR3-N from Dualsystems Biotech.

Unless indicated otherwise, MG1655 chromosomal DNA was used as template in amplification reactions. Sites of interest (e.g. relevant restriction sites) are underlined in primer sequences.

Plasmid pCH311 [P_{lac}::*zipA-rfp*] encodes a fusion of ZipA to mCherry RFP, and its *rfp* ORF is codon-optimized for *E.coli*. To create it, the *rfp* ORF was amplified from pJ1:G01080 (kind gift from Ken Marians) using primers 5'-AGGGGATCCGGAATTCATGGTTTCCAAGGGCGAGGAGGATAAC-3' and 5'-TTACGGCATGCGTCGACTTATTTGTACAGCTCATCCATGCC-3'. The product was treated

with *Bam*HI and *Sph*I, and the 734 bp fragment was used to replace the 746 bp *Bam*HI-*Sph*I fragment of pCH151 [P_{lac}::*zipA-gfp*].

pCH314 [*ori*R6K *rfp frt-cat-fr*] was obtained by replacing the 766 bp *Bam*HI-*Sal*I fragment of pTB24 [*ori*R6K *gfp frt-cat-fr*] (see below) with the 724 bp *Bam*HI-*Sal*I fragment of pCH311.

For pCH356 [P_{lac}::*mreB'-t18-'mreB*], the *t18* portion of *Bordetella pertussis* adenylate cyclase (*cyaA*) was amplified from pUT18 using primers 5'-GCCGCCTCGAGCGCCGCCAGCGAGGCCACGGGCGGCCTG-3' and 5'-GAGAGGCGCGCCAGAGCGTTCCACTGCGCCCAGCGACGGCCG-3'. The product was digested with *Xho*I and *Asc*I and the resulting 536 bp fragment was used to replace the 17 bp *Xho*I-*Asc*I fragment of pFB259. [P_{lac}::*mreB'-linker-'mreB*] (see below). Plasmid pCH356 encodes a MreB'-T18-'MreB sandwhich fusion (MreB-$T18^{SW}$) that harbors the peptide SGSS-[T18]-SGAPG between G228 and D229 of MreB.

For pCH357 [P_{lac}::*mreB'-t25-'mreB*], the *t25* portion of *B.pertussis cyaA* was amplified from pKT25 using primers 5'- GTACCTCGAGCATGCAGCAATCGCATCAGGCTGGTTACGC -3' and 5'- TAGAGGCGCGCCAGATGCAGCCCGCCGCGTGCGCGCCAG -3'. The product was digested with *Xho*I and *Asc*I and the resulting 689 bp fragment was used to replace the 17 bp *Xho*I-*Asc*I fragment of pFB259. [P_{lac}::*mreB'-linker-'mreB*]. Plasmid pCH357 encodes a MreB'-T25-'MreB sandwhich fusion (MreB-$T25^{SW}$) that harbors the peptide SGSS-[T25]-SGAPG between G228 and D229 of MreB.

For pCH358 [*aph* P_{lac}::*t25-rodZ*], *rodZ* was amplified from pFB237 (see below) with primers 5'- ATACGGCCATTACGGCCATGAATACTGAAGCCACGCACG-3' and 5'-ATGCGGCCGAGGCGGCCTTACTGCGCCGGTGATTGTTCG-3'. The product was digested with *Sfi*I and the 1027 bp fragment was used to replace the 27 bp *Sfi*I fragment of pBT3-N. This resulted in pCH325 [P_{cyc1}::*lexA-vp16-cub-rodZ*], which served as template to amplify *rodZ* with primers 5'- GTACTCTAGAGGCCATTACGGCCATGAATACTGAAGCC-3' and 5'-GTACGAATTCGGCCGAGGCGGCCTTACTGCGC-3'. The product was digested with *Xba*I and *EcoR*I, and the 1046 bp fragment was used to replace the 32 bp *Xba*I-*EcoR*I fragment of pKT25, yielding pCH358.

Plasmids pCH363 [*bla lacI*^{q} P_{lac}::*lacZ'-t18*] and pCH364 [*bla lacI*^{q} P_{lac}::*t18*-] were created to serve as general vectors for the expression of fusions to the T18 domain of *B.pertussis* adenylate cyclase. These pMLB1115-derivatives allow better control of the expression level of T18-fusions than pUT18 and pUT18C, as they encode LacI^q in cis and their copy number is lower. For pCH363, the *t18* portion of pUT18 was amplified, using primers 5'-CGCCAAGCTTGCATGCCTGCAGG-3' and 5'-AGCTGCTCAGCTTATATCGATTGGCGTTCCACTGC-3'. The product was treated with *Hind*III and *Blp*I, and the 596 bp fragment was ligated to the 4551 bp *Hind*III-*Blp*I fragment of pMLB1115. For pCH364, the *t18* portion of pUT18C was amplified, using primers 5'-TACGCCAAGCTTAGCCGCCAGCGAGG-3' and 5'-GACTCGTACGTTATATCGATGAATTCGAGCTCGG-3'. The product was treated with *Hind*III and *BsiW*I, and the 589 bp fragment was ligated to the 4792 bp *Hind*III-*BsiW*I fragment of pMLB1115.

To obtain pCH371 [P_{lac}::*t18-rodZ*], the 1046 bp *Xba*I-*EcoR*I fragment of pCH358 was used to replace the 27 bp *Xba*I-*EcoR*I fragment of pCH364.

For pCH375 [P_{lac}::*mreB'-t25-'mreB*], the 2604 bp *Xba*I-*Cla*I fragment of pCH357 was used to replace the 721 bp *Xba*I-*Cla*I fragment of pKNT25. pCH375 is a pACYC-type plasmid that encodes the same MreB'-T25-'MreB sandwhich fusion (MreB-T25^{SW}) as the ColE1-type pCH357.

To create pCH378 [P_{lac}::*t25-mreC*], *mreC* was amplified with primers 5'-CAGTGGCCATTACGGCCATGAAGCCAATTTTTAGCCG-3' and 5'-ATCGGGCCGAGGCGGCCTTATTGCCCTCCCGGCGCACGC-3'. The product was digested with *Sfi*I and the 1117 bp fragment was used to replace the 27 bp *Sfi*I fragment of pBT3-N, resulting in pCH331 [P_{cyc1}::*lexA-vp16-cub-mreC*]. The 1117 bp *Sfi*I fragment of pCH331 was next used to replace the 1027 bp *Sfi*I fragment of pCH358, yielding pCH378.

For pCH379 [P_{lac}::*t25-pbpA*], *pbpA* was amplified with primers 5'-GCATGGCCATTACGGCCATGAAACTACAGAACTCTTTTCGCG-3' and 5'-TGCAGGCCGAGGCGGCCTTAATGGTCCTCCGCTGCGGC-3'. The product was digested with *Sfi*I and the 1915 bp fragment was used to replace the 27 bp *Sfi*I fragment of pBT3-N, resulting

in pCH351 [P_{cyc1}::*lexA-vp16-cub-pbpA*]. The 1915 bp *Sfi*I fragment of pCH351 was then used to replace the 1027 bp *Sfi*I fragment of pCH358, yielding pCH379.

For pCH382 [P_{lac}::*t18-mreC*], the 1117 bp *Sfi*I fragment of pCH331 was used to replace the 1027 bp *Sfi*I fragment of pCH371.

For pCH383, [P_{lac}::*t18-pbpA*], the 1915 bp *Sfi*I fragment of pCH351 was used to replace the 1027 bp *Sfi*I fragment of pCH371.

To obtain pCH384 [P_{lac}::*t25-mreD*], *mreD* was amplified using primers 5'-GTCAGGCCATTACGGCCATGGCGAGCTATCGTAGCCAG -3' and 5'-CAGTGGCCGAGGCGGCCTTATTGCACTGCAAACTGCTGACG-3'. The product was digested with *Sfi*I and the 502 bp fragment was used to replace the 27 bp *Sfi*I fragment of pBT3-N, yielding pCH335 [P_{cyc1}::*lexA-vp16-cub-mreD*]. The 502 bp *Sfi*I fragment of pCH335 was next used to replace the 1027 bp *Sfi*I fragment of pCH358, resulting in pCH384.

For pCH385 [P_{lac}::*t25-rodA*], *rodA* was amplified using primers 5'-CTGAGGCCATTACGGCCATGACGGATAATCCGAATAAAAAAACATTCTGG -3' and 5'-GATCGGCCGAGGCGGCCTTACACGCTTTTCGACAACATTTTCCTG-3'. The product was digested with *Sfi*I and the 1126 bp fragment was used to replace the 29 bp *Sfi*I fragment of pPR3-N, yielding pCH343 [P_{CYC1}::*nubG-ha-rodA*]. The 1126 bp *Sfi*I fragment of pCH343 was next used to replace the 1027 bp *Sfi*I fragment of pCH358, resulting in pCH385.

To obtain pCH386 [P_{lac}::*t18-mreD*], the 502 bp *Sfi*I fragment of pCH335 was used to replace the 1027 bp *Sfi*I fragment of pCH371.

For pCH387 [P_{lac}::*t18-rodA*], the 1126 bp *Sfi*I fragment of pCH343 was used to replace the 1027 bp *Sfi*I fragment of pCH371.

For pCH390 [P_{lac}::*t25-rodZ*(83-337)], a portion of pCH348 was amplified with 5'-GCATGGCCATTACGGCCCTCGAGAAGCAGGCTCCACTTCGG -3' and 5'-ATGCGGCCGAGGCGGCCTTACTGCGCCGGTGATTGTTCG-3'. The product was treated with *Sfi*I, and the 781 bp fragment was used to replace the 1027 bp *Sfi*I fragment of pCH358.

To obtain pCH393 [P_{lac}::*t18-rodZ*(1-84)-*malF*(1-39)-*rfp*], a portion of pFB306 [P_{lac}::*rodZ*(1-84)-*malF*(1-39)-*rfp*] (see below) was amplified with primers 5'-GTACTCTAGAGGCCATTACGGCCATGAATACTGAAGCC-3' and 5'-AGCTGGCCGAGGCGGCCTTATTTGTACAGCTCATCCATGC-3'. The product was digested with *Sfi*I and the 1108 bp fragment was used to replace the 1027 bp *Sfi*I fragment of pCH371.

For pCH406 [P_{lac}::*t18-rodZ*(1-84)-*malF*(1-14)-*rodZ*(111-337)], a portion of pYT25 was amplified with primers 5'- ATACGGCCATTACGGCCATGAATACTGAAGCCACGCACG-3' and 5'- ATGCGGCCGAGGCGGCCTTACTGCGCCGGTGATTGTTCG-3'. The product was digested with *Sfi*I and the 1033 bp fragment was used to replace the 502 bp *Sfi*I fragment of pCH386, yielding pCH396 [P_{lac}::*t18-rodZ*(1-97)-*malF*(2-14)-*rodZ*(111-337)]. The 1479 bp *Apa*I-*Nco*I fragment of pCH393 was then used to replace the 1512 bp *Apa*I-*Nco*I fragment of pCH396, resulting in pCH406.

For pCH414 [P_{lac}::*t18-rodZ*(83-337)], the 781 bp *Sfi*I fragment of pCH390 was used to replace the 1027 bp *Sfi*I fragment of pCH371.

To create pFB105 [P_{T7}::*t-mreB-h*], *mreB* was amplified with primers 5'-CTTGGATCCTTGAAAAAATTTCGTGGCATGTTTTC-3' and 5'-CGCTTCTCGAGCTCTTCGCTGAACAGGTCGCCG-3'. The product was treated with *Bam*HI and *Xho*I, and the 1044 bp fragment was ligated to similarly digested pET21a. Plasmid pFB105 encodes a 39.3 kD derivative of MreB (T-MreB-H) in which the starting methionine has been replaced with the T7.tag peptide (MASMTGGQQMGRGS), and the hexahistidine tag LEH_6 has been appended to its C-terminal residue.

Plasmid pFB114 [P_{lac}::*gfp-mreB*(5-347)] was obtained by replacing the 538 bp *Xba*I-*Kpn*I fragment of pCH214 [P_{lac}::*mreB*] with the 1278 bp *Xba*I-*Kpn*I fragment of pDB366 [P_{lac}::*gfp-mreB*(5-347)*, mreC, mreD, yhdE*].

To construct pFB184 [*ori*F P_{lac}::*sdiA*::*lacZ*], pCX16 [*sdiA*] was used as template to amplify *sdiA* with primers 5'-GGAATTCAAG***AAGGAG***ATTTTACTATGCAGGATAAGG-3' and 5'-GAGCGTGTCGACTCAAATTAAGCCAGTAGCGG-3'. The product was treated with *Eco*RI and *Sal*I and the 746 bp fragment was ligated to the 13027 bp *Eco*RI-*Sal*I fragment of pRC7. Use of

the strong T7 *gene*10 ribosome binding site (bold italics) ensured a sufficient level of SdiA production from this mini-F derivative.

For plasmid pFB206 [P_{BAD}::*mreCD*], the 1616 bp *Xba*I-*Xho*I fragment of pFB124 was used to replace the 2728 bp *Xba*I-*Xho*I fragment of pFB174.

To obtain pFB214 and pFB216 [P_{tac}::*mreB*], *mreB* was amplified using primers 5'-CGACTCTAGACAGCTTTCAGGATTATCCCTTAGTATG-3' and 5'-GCAAAAGCTTACTCTTCGCTGAACAGGTCGCC-3'. The product was treated with *Xba*I and *Hind*III and the 1072 bp fragment was used to replace the 611 bp *Xba*I-*Hind*III fragment of pDR144 [P_{lac}::*sfiA*], yielding pFB209 [P_{lac}::*mreB*]. The 1148 bp *Eco*RI-*Hind*III fragment of pFB209 was next ligated to similarly digested pJF188EH, yielding pFB214. Plasmid pFB216 was obtained by ligation of the 2688 bp *Nru*I-*Hind*III fragment of pFB214 with the 4711 bp *Nru*I-*Hind*III fragment of pFB174.

For plasmids pFB233 [P_{lac}::*rodZ*(1-319)], pFB234 [P_{lac}::*ispG*], and pFB235 [P_{lac}::*rodZ ispG*], PCR products were treated with *Xba*I and *Hind*III and resulting fragments (1076, 1165, and 2221 bp, respectively) were used to replace the 1294 bp *Xba*I-*Hind*III fragment of pCH233 [P_{lac}::*gfp-mreD*]. Primers used were: 5'-GCTCTAGAGGTGAGCATGATGGTTCACCGGC-3' and 5'-CCCAAGCTTTTACTGCGCCGGTGATTGTTCGGC-3' (pFB233), 5'-GCTCTAGACACCGGCGCAGTAACAGACGGG-3' and 5'-CCCAAGCTTTTATTTTTCAACCTGCTGAACGTCAATTCGACGCG-3' (pFB234), and GCTCTAGAGGTGAGCATGATGGTTCACCGGC-3'and CCCAAGCTTTTATTTTTCAACCTGCTGAACGTCAATTCGACGCG-3 (pFB235).

For plasmid pFB237 [P_{lac}::*gfp-t-rodZ*], *rodZ* was amplified with primers 5'-CGCGGATCCATGAATACTGAAGCCACGCACGACC-3' and 5'-CCCAAGCTTTTACTGCGCCGGTGATTGTTCGGC-3'. The product was treated with *Bam*HI and *Hind*III and the resulting 1020 bp fragment was used to replace the 1039 bp *Bam*HI-*Hind*III fragment of pFB114.

Plasmid pFB244 [P_{tac}::*rodZ*(1-319)] was made by replacing the 1072 bp *Xba*I-*Hind*III fragment of pFB181 with the 1076 bp *Xba*I-*Hind*III fragment from pFB233. A mutation in pFB233 and pFB244 that resulted in an early stop codon after codon 319 was repaired by replacing the

511 bp *Sal*I-*HInd*III from each plasmid with the 511 bp *Sal*I-*Hind*III fragment from pFB237. This yielded plasmids pFB290 [P_{lac}::*rodZ*] and pFB291 [P_{tac}::*rodZ*], respectively.

For plasmid pFB254 [P_{T7}::*h-sumo-rodZ*(1-319*)*], *rodZ* was amplified from pFB233 with primers 5'-GGTGGTTGCTCTTCCGGTATGAATACTGAAGCCACGCACGACC-3' and 5'-CCGCTCGAGTTACTGCGCCGGTGATTGTTCGGC-3'. The product was digested with *Sap*I and *Xho*I and the 1018 bp fragment was ligated to similarly digested pTB146 [P_{T7}::*h-sumo*].

To create pFB259 [P_{lac}::*mreB'-linker-'mreB*], pFB209 was used as template to amplify *mreB* codons 1 through 228 with primers 5'-TCACAAAGCTTACAGCTATGACCATGATTACG-3' and 5'-CCAGAGCATGCGCTCGAGCCAGAACCCGGATAAGCCGAACCGATTTCG-3' in reaction 1, and codons 229 thorugh 367 with primers 5'-TCGAGCGCATGCTCTGGCGCGCCGGGCGATGAAGTCCGTGAAATCG-3' and 5'-GACGTTGTAAAACGACGGCCAGTG-3' in reaction 2. The product of reaction 1 was digested with *Xba*I and *Sph*I to yield a 730 bp fragment, and that of reaction 2 with *Sph*I and *Hind*III to yield a 375 bp fragment. Three-way ligation of both fragments to the 7639 bp *Xba*I-*Hind*III fragment of pFB209 resulted in pFB259. The linker encodes an in-frame peptide (SGSSACSGAPG) between G228 and D229 of MreB.

For plasmid pFB262 [P_{lac}::*mreB'-rfp-'mreB*], codon-optimized mCherry *rfp* was amplified from plasmid pCH314 with primers 5'-GGTTCTGGCTCGAGCATGGTTTCCAAGGGCGAGGAGGATAAC-3' and 5'-CATCGCCCGGCGCGCCAGATTTGTACAGCTCATCCATGCCACC-3'. The product was treated with *Xho*I and *Asc*I and the resulting 719 bp fragment was used to replace the 17 bp *Xho*I-*Asc*I fragment of pFB259. Plasmid pFB262 encodes a functional MreB'-RFP-'MreB sandwhich fusion (MreB-RFP^{SW}) that harbors the in-frame peptide SGSS-[RFP]-SGAPG between G228 and D229 of MreB.

For plasmid pFB273 [oriR6K *att*HK022 P_{lac}::*gfp-t-rodZ*], the 1020 bp *Bam*HI-*Hind*III fragment of pFB237 was ligated to the 4257 bp *Bam*HI-*Hind*III fragment of pTB183 [oriR6K *att*HK022 P_{lac}::*gfp-t-zapA*] (see below).

Plasmid pFB274 [oriR6K *att*HK022 P_{lac}::*gfp-Δ30-parB*] was obtained by ligation of the 1145 bp *Mfe*I-*Hind*III fragment of pALA2705 to the 4070 bp *Mfe*I-*Hind*III fragment of pTB183.

To create pFB285 [oriR6K *att*HK022 P_{lac}::*gfp-t-rodZ*(1-111)-*r*], a portion of pFB237 [P_{lac}::*gfp-t-rodZ*] was amplified with primers 5'-TTAGGCACCCCAGGCTTTACAC-3' and 5'-CCGCTCGAGTTATCGGCCGTCGCGTTTTTTGCGGCGTTTACCGAGGG-3'. The product was treated with *Xba*I and *Xho*I and the 1118 bp fragment was ligated to the 7662 bp *Xba*I-*Xho*I fragment of pCH233 [P_{lac}::*gfp-t-mreD-le*], yielding pFB252 [P_{lac}::*gfp-t-rodZ*(1-111)-*r*]. The 1141 bp *Xba*I-*Hind*III fragment of pFB252 was next ligated to the 3484 bp *Xba*I-*Hind*III fragment of pTB183, yielding pFB285.

Construction of pFB289 [oriR6K *att*HK022 P_{lac}::*gfp-t-rodZ*(1-111)-*r-malF*(17-39*)-rfp*] involved multiple intermediate constructions. The 1346 bp *Bam*HI-*Pst*I fragment of pET21a was ligated to the 4213 bp *Bam*HI-*Pst*I fragment of pDB311 [P_{T7}::*hfkt-minE*], yielding pDB328 [P_{T7}::*hfkt*]. A portion of *mreC* was amplified, using primers 5'-CGCGGATCCATCCGTACTTATATGGATACC-3' and 5'-CCCCAAGCTTCTATTGCCCTCCCGGCGC-3'. The product was digested with *Bam*HI and *Hind*III and the resulting 999 bp fragment was ligated to the 5534 bp *Bam*HI-*Hind*III fragment of pDB328, yielding pFB212 [P_{T7}::*hfkt-mreC*(38-367)]. The latter was treated with *Xba*I and *Xho*I and the 1208 bp product was ligated to the 7762 bp *Xba*I-*Xho*I fragment of pCH235 [P_{lac}::*mreD-le*] to yield pFB221 [P_{lac}::*hfkt-mreC*(38-367)]. Next, a portion of *malF* was amplified with primers 5'-GCTCTAGAGAAAGCCTTATCCGTCCTGG-3' and 5'-CGGGATCCTTCCCCTTGTGCGTAC-3'. The product was digested with *Xba*I and *Bam*HI and the 159 bp product was ligated to the 8676 bp fragment of similarly treated pFB221, resulting in pFB225 [P_{lac}::*malF*(1-39)-*mreC*(38-367)]. To eliminate an undesired *Eag*I site from the latter, it was treated with *Hind*III and the 8797 bp fragment was recircularized to yield pFB240 [P_{lac}::*malF*(1-39)-*mreC*(38-367)]. A desired *Eag*I site (Guzman et al., 1997) was then engineered into plasmid pFB240 by the Quichchange method using oligo 5'-CATTGGTGGCAAAGCGACGCCGGCCGATGGTCAGTGCTAGGTCTGCTCGG-3' and its reverse complement (*Eag*I site underlined), yielding plasmid pFB243 [P_{lac}::*malF*(1-39)-*mreC*(38-367)]. Note that introduction of the *Eag*I site in pFB243 also introduced two inocuous MalF codon changes (L11G and K12R), as was described before (Guzman et al., 1997). A portion of pFB243 was next amplified using primers 5'-GCTCTAGAGAAAGCCTTATCCGTCCTGG-3' and 5'-CCGGATCCTCCCCTTGTGCGTAC-3'. The product was treated with *Xba*I and *Bam*HI, and the 158 bp fragment was used to replace the 1031 bp *Xba*I-*Bam*HI fragment of pCH311 [P_{lac}::*zipA-rfp*], giving rise to pFB250 [P_{lac}::*malF*(1-39)-*rfp*]. Subsequently, a portion of plasmid pFB237 [P_{lac}::*gfp-t-rodZ*] was amplified with primers 5'-TTAGGCACCCCAGGCTTTACAC-3' and

5’-CCGCTCGAGTTATCGGCCGTCGCGTTTTTTGCGGCGTTTACCGAGGG-3’ and the product was treated with *Xba*I and *Eag*I. The resulting 1108 bp fragment was ligated to the 8450 bp fragment of similarly treated pFB250, yielding pFB264 [P_{lac}::*gfp-t-rodZ*(1-111)-*r-malF*(17-39)-*rfp*]. Finally, plasmid pFB289 was obtained by treating pFB264 with *Xba*I and *Sal*I and ligating the resulting 1907 bp fragment with the 3490 bp fragment of similarly treated pTB183.

The construction of plasmids pFB290 [P_{lac}::*rodZ*] and pFB291 [P_{tac}::*rodZ*] is detailed further above.

For pFB293 [oriR6K *att*HK022 P_{lac}::*gfp-t-malF*(2-14)-*gr-rodZ*(111-337)], a portion of pFB233 [P_{lac}::*rodZ*(1-319)] was amplified using primers 5’-GCGACGCCGGCCGAGGCTGGCTGATGACCTTCACTTGGC-3’ and 5’-CCGCTCGAGTTACTGCGCCGGTGATTGTTCGGC-3’. The product was digested with *Eag*I and *Xho*I and the 691 bp fragment was ligated to the 8479 bp *Eag*I-*Xho*I fragment of pCH310 [P_{lac}::*gfp-malF*(2-39)-*ftsN*(55-123)] (a plasmid that will be detailed elsewhere), yielding pFB261 [P_{lac}::*gfp-t-malF*(2-14)-*gr-rodZ*(111-319)]. The 997 bp *Xba*I-*Sal*I fragment of pFB261 was next used to replace the 1282 bp *Xba*I-*Sal*I fragment of pFB273 [oriR6K *att*HK022 P_{lac}::*gfp-t-rodZ*], resulting in pFB293.

To obtain pFB299 [P_{tac}::*mreB rodZ*], a portion of pFB214 [P_{tac}::*mreB*] was amplified with primers 5’-TCATCGGCTCGTATAATGTGTGG-3’ and 5’-CACCTCTAGATTACTCTTCGCTGAACAGGTCGCC-3’. The product was treated with *Xba*I and the resulting 1074 bp fragment was inserted in the *Xba*I site of pFB291 [P_{tac}::*rodZ*].

Plasmid pFB309 [P_{syn135}::*gfp-rodZ*] produces GFP-RodZ under control of a synthetic constitutitive promotor, and was made in several steps. Ligation of the 1109 bp *Xba*I-*Sal*I fragment of pTB97 to the 2631 bp *Xba*I-*Sal*I fragment of pCAH63 [oriR6K *attλ* P_{syn1}] resulted in plasmid pEZ1 [oriR6K *attλ* P_{syn1}::*gfp-zapA*]. The -35 promoter element of the P_{syn1} promotor in pEZ1 was next modified by the QuickChange procedure (Stratagene), using oligo 5’-GAATTCTAGGCTTTACACTTTATGCTTCCGGC-3’ and its reverse complement, resulting in a T to C mutation (underlined) and yielding pEZ4 [oriR6K *attλ* P_{syn135}::*gfp-zapA*]. The 1163 bp *Eco*RI-*Sal*I fragment of pEZ4 was subsequently used to replace the 33 bp *Eco*RI-*Sal*I fragment of pZC100, giving rise to pCH362 [P_{syn135}::*gfp-zapA*]. Finally, the 1793 bp *Xba*I-*Hind*III fragment of pFB237 was used to replace the 1127 bp *Xba*I-*Hind*III fragment of pCH362, yielding pFB309.

Plasmid pFB310 [$P_{\lambda R}$::*mreB'-rfp-'mreB*] was made in two steps. First, the 1105 bp *Xba*I-*Hind*III fragment from pFB259 [P_{lac}::*mreB'-linker-'mreB*] was ligated to the 4164 bp *Xba*I-*Hind*III fragment of pTB188 [$P_{\lambda R}$::*ftsZ*] to yield plasmid pFB305 [$P_{\lambda R}$::*mreB'-linker-'mreB*]. Then, the 719 bp *Xho*I-*Asc*I fragment of pFB262 [P_{lac}::*mreB'-rfp-'mreB*] was ligated to the 5252 bp *Xho*I-*Asc*I fragment of pFB305 to yield pFB310.

For plasmid pFB312 [oriR6K *att*HK022 P_{lac}::*gfp-t-rodZ*(83-138)-*rfp*], a portion of pYT27 (see below) was amplified with primers 5'-TTAGGCACCCCAGGCTTTACAC-3' and 5'-CGCGAGATCTGGAGCTTTGCGGTCTTGCCACCACC-3'. The product was treated with *Xba*I and *Bgl*II and the 949 bp fragment was ligated to the 4214 bp *Xba*I-*Bam*HI fragment of pYT22 (see below).

Plasmid pFB319 [*ori*R6K *att*HK022 P_{lac}::*gfp-t-rodZ*(1-84)-*malF*(1-39)-*rfp*] was made in several steps. A portion of pFB290 [P_{lac}::*rodZ*] was amplified with primers 5'-TTAGGCACCCCAGGCTTTACAC-3' and 5'-CGCGCCATGGTTTCCAGCCCTGGCAGCAGTTCTTC-3'. The product was treated with *Xba*I and *Nco*I and the 315 bp fragment was ligated to the 8493 bp *Xba*I-*Nco*I fragment of pFB250 [P_{lac}::*malF*(1-39)-*rfp*]. This resulted in plasmid pFB306 [P_{lac}::*rodZ*(1-84)-*malF*(1-39)-*rfp*], which was treated with *Xba*I and *Nru*I. The 8679 bp product was then ligated to the 846 bp *Xba*I-*Nru*I fragment of pFB237 [P_{lac}::*gfp-t-rodZ*], yielding plasmid pFB311 [P_{lac}::*gfp-t-rodZ*(1-84)-*malF*(1-39)-*rfp*]. Finally, the 1874 bp *Xba*I-*Sal*I fragment of pFB311 was ligated to the 3490 bp *Xba*I-*Sal*I fragment of pTB183 to yield pFB319.

Plasmid pFB321 [*ori*R6K *att*HK022 P_{lac}::*gfp-t-rodZ*(1-84)-*malF*(1-14)-*rodZ*(111-337)] was made by ligation of the 1807 bp *Apa*I-*Ngo*MIV fragment from pFB311 to the 3443 bp *Apa*I-*Ngo*MIV fragment of pFB293.

For pTB22 [*ori*R6K *frt-cat-fr*], the *frt-cat-frt* cassette of pKD3 was amplified using primers 5'-CTCTGAGCTCGACTACAAGGACGATGACGACAAATAAATGAATATCCTCCTTAGTTCC-3' and 5'-CTCTAGATCTGTGTAGGCTGGAGCTGCTTCG-3' . The product was treated with *Sac*I and *Bgl*II, and the 1061 bp fragment was used to replace the 1371 bp *Sac*I-*Bgl*II fragment of pUNI10 [*ori*R6K *aph*].

pTB24 [*ori*R6K *gfp frt-cat-fr*] was obtained by replacing the 51 bp *Xho*I-*Sal*I fragment of pTB22 with the 787 bp *Xho*I-*Sal*I fragment of pDR123 [aadA::*minDE-gfp*].

Plasmids pTB97, pTB98, pTB183, and pTB222 were used as integrative CRIM vectors, and were derived from pAH68 [*ori*R6K *att*HK022 *bla*] in several steps. Fragments containing the R6K origin, the *att*HK022 site, and a portion of the *bla* gene were amplified from pAH68 using the forward primers 5'- TATCGATCTCACGATAATATCCGGGTAGGCG-3' or 5'- AGCTTATCGATCTCACGATAATATCCGGGTAGGCG-3' and the reverse primer 5'- GGGCAAGAGCAACTCGGTCGC-3'. The resulting 1638 bp and 1642 bp fragments were mixed, incubated in a boiling water bath, and cooled, to generate a population of fragments with a *Hind*III overhang (underlined) on one end. The fragments were digested with *Sca*I (internal to fragment) and ligated either to the 3009 bp *Sca*I-*Hind*III fragment of pCH268 [P_{lac}::*gfp-zapA*], yielding pTB97 [*ori*R6K *att*HK022 *bla lacI*^{q} P_{lac}::*gfp-zapA*], or to the 3673 bp *Sca*I-*Hind*III fragment of pCH151 [P_{lac}::*zipA-gfp*], yielding pTB98 [*ori*R6K *att*HK022 *bla lacI*^{q} P_{lac}::*zipA-gfp*]. An undesired *Hind*III site in the *ori*R6K region of pTB97 was changed to AACCTT using the Quickchange method (Stratagene) and the mutagenic primers 5'- CCGTTAAACCTTAAAACCTTTAAAAGCCTTATAT-3' and its reverse complement, resulting in pTB183 [*ori*R6K *att*HK022 *bla lacI*^{q} P_{lac}::*gfp-zapA*]. The 1779 bp *Xba*I-*Hind*III fragment of pTB98 was then used to replace the 1115 bp *Xba*I-*Hind*III fragment of pTB183, resulting in pTB222 [*ori*R6K *att*HK022 *bla lacI*^{q} P_{lac}::*zipA-gfp*].

Plasmid pTB145 [P_{T7}::*h-ulp*1(403-621)] encodes a His_6-tagged version of the catalytically active domain of yeast SUMO-protease. To construct it, a portion of *ulp*1 was amplified from *Saccharomyces cerevisiae* SC288 genomic DNA (Invitrogen), using primers 5'- GGTGGTGCTAGCGGACTTGTTCCTGAATTAAATGAAAAAGACG-3' and 5'- GGTGCTCGAGTTATTTTAAAGCGTCGGTTAAAATCAAATGG-3'. The product was treated with *Nhe*I and *Xho*I, and the resulting 669 bp fragment was ligated to the 5399 bp *Nhe*I-*Xho*I fragment of pCH260 [P_{T7}::*h-t*].

For pTB146 [P_{T7}::*h-sumo*], the SUMO gene *smt3* (*sumo*) was amplified from *S.cerevisiae* SC288 genomic DNA with primers 5'- GGTGGTGCTAGCGGATCGGACTCAGAAGTCAATCAAGAAGC-3' and 5'- GGTAAGAGCTCTGCTCTTCTACCACCAATCTGTTCTCTGTGAGCC-3' . The product was treated with *Nhe*I and *Sac*I, and the 313 bp fragment was ligated to the 5423 bp *Nhe*I-*Sac*I

fragment of pCH260 [P_{T7}::*h-t*], yielding pTB144 [P_{T7}::*h-sumo*]. To obtain a vector with a unique *Sap*I cloning site, the 411 bp *Xba*I-*Xho*I fragment of pTB144 was next ligated to the 5755 bp *Xba*I-*Xho*I fragment of pTYB12, resulting in pTB146.

To construct pYT19 [P_{lac}::*rodZ*(1-97)-*malF*(2-39)-*rfp*], a portion of *rodZ* was amplified with primers 5'-GCTCTAGAGGTGAGCATGATGGTTCACCGGC-3' and 5'-GCCGCTCGAGTCCCATGGGCGCAACTTTTGCAGCCC-3'. The product was treated with *Xba*I and *Nco*I, and the 348 bp fragment was used to replace the 40 bp *Xba*I-*Nco*I fragment of pFB250 [P_{lac}::*malF*(1-39)-*rfp*].

Plasmid pYT22 [*ori*R6K *att*HK022 P_{lac}::*gfp-t-rodZ*(1-138)-*rfp*] was made in several steps. A portion of pFB233 [P_{lac}::*rodZ*(1-319)] was amplified with primers 5'-GCTCTAGAGGTGAGCATGATGGTTCACCGGC-3' and 5'-CGGGATCCGGAGCTTTGCGGTCTTGCCACCACC-3' and the product was treated with *Xba*I and *Bam*HI. The resulting 478 bp fragment was ligated to the 8375 bp *Xba*I-*Bam*HI fragment of pCH311 [P_{lac}::*zipA-rfp*], yielding pFB249 [P_{lac}::*rodZ*(1-138)-*rfp*]. The 1202 bp *Xba*I-*Sal*I fragment of pFB249 was next used to replace the 1109 bp *Xba*I-*Sal*I insert of pTB183, resulting in pYT17 [*ori*R6K *att*HK022 P_{lac}::*rodZ*(1-138)-*rfp*]. Finally, the 129 bp *Xba*I-*Nru*I fragment of pYT17 was replaced with the 846 bp *Xba*I-*Nru*I fragment of pFB237 [P_{lac}::*gfp-t-rodZ*], yielding pYT22.

For pYT23 [P_{lac}::*gfp-t-rodZ*(1-97)-*malF*(2-39)-*rfp*], the 846 bp *Xba*I-*Nru*I fragment of pFB237 [P_{lac}::*gfp-t-rodZ*] was used to replace the 129 bp *Xba*I-*Nru*I fragment of pYT19.

To construct pYT25 [P_{lac}::*gfp-t-rodZ*(1-97)-*malF*(2-14)-*rodZ*(111-337)], the 691 bp *Eag*I-*Hind*III fragment of pFB293 [oriR6K *att*HK022 P_{lac}::*gfp-t-malF*(2-14)-*gr-rodZ*(111-337)] was ligated to the 8747 bp *Eag*I-*Hind*III fragment of pYT23.

Construction of plasmid pYT27 [oriR6K *att*HK022 P_{lac}::*gfp-t-rodZ*(83-337)] involved several steps. A portion of *rodZ* was amplified with primers 5'-CGGGATCCTCGAGAAGCAGGCTCCACTTCGGGCTGC-3' and 5'-CCCAAGCTTTTACTGCGCCGGTGATTGTTCGGC-3' and the product was digested with *Bam*HI and *Hind*III. The resulting 774 bp fragment was ligated to the 7717 bp *Bam*HI-*Hind*III fragment of pJE42 [P_{lac}::*t-dicB-gfp*], yieding pYT1 [P_{lac}::*rodZ*(83-337)]. The 768 bp *Xho*I-*Hind*III fragment from pYT1 was subsequently ligated to the 7719 bp *Xho*I-*Hind*III fragment of pFB266

[P_{lac}::*t-λcI*(93-237)] (a plasmid that will be detailed elsewhere), resulting in pYT9 [P_{lac}::*t-rodZ*(83-337)]. Next, the 773 bp *Xba*I-*BamH*I fragment of pTB183 was ligated to the 8409 bp *Xba*I-*BamH*I fragment of pYT9 to yield plasmid pYT24 [P_{lac}::*gfp-t-rodZ*(83-337)]. Finally, pYT27 was obtained by ligation of the 1547 bp *Xba*I-*Hind*III fragment of pYT24 to the 3484 bp *Xba*I-*Hind*III fragment of pTB183.

Phages λFB234 and λFB237 were generated by crossing λNT5 with pFB234 and pFB237, respectively, as described previously (de Boer et al., 1989).

***E. coli* strains**.

The most relevant strains used in this study are listed in Table S2.

Most knock-out strains were constructed by λ Red recombineering, using pKD3 [*frt cat frt*] or pKD13 [*frt aph frt*] as templates for the generation of mutagenic recombineering fragments with evictable selection markers (Datsenko and Wanner, 2000; Yu et al., 2000). Homologies to chromosomal DNA targets are underlined in the sequences of the primers that were used to amplify the corresponding recombineering fragments.

Strain FB54/pTB63 [*rodZ*::EzTnkan/ *ftsQAZ*] was obtained by P1-mediated transduction (transduction, for short) of the *rodZ*::EzTnkan allele from Rod2353/pFB184 to TB28/pTB63.

For FB57 [*yhdE*<>*cat*], the *cat* cassette of pKD3 was amplified with primers 5'-ATGACTTCTCTGTATTTAGCTTCCGGTTCTCCGCGTCGTCAGGAGTTACTGTGTAGGCTGGAGCTGCTTCG-3' and 5'-CATAGCCCGCGATGTCTTCGTCTGTTAACGTTCTGAAAGTCACATCGGTGTTAGTTCCTATTCCGAAGTTCC-3', and the fragment was recombined with the chromosome of TB10. Recombinants were selected at 30°C on LB agar supplemented with 10 μg/ml Cam.

To construct FB58/pCX16 [*rodZ*<>*aph*/*sdiA*] and FB59/pCX16 [*rodZ*155<>*aph*/*sdiA*], the *aph* cassette of pKD13 was amplified with primer sets 5'-CATGATGGTTCACCGGCATCTCAATTCTCATTTAAACGTACCTGCAGCGAGTGTAGGCTGGAGCTGCTTC-3' and 5'-CCGCTAAACAATTTTTTACCGGTAGCATCAGTGACCTCCAGCCAGCAATCATTCCGGGGAT

CCGTCGACC-3' (for *rodZ*<>*aph*), and 5'-
AGCAGGAAGAGATCACCACTATGGCCGATCAATCTTCGGCGGAACTGAGCTAAGTGTAGG
CTGGAGCTGCTTC-3' and 5'-
CCGCTAAACAATTTTTTACCGGTAGCATCAGTGACCTCCAGCCAGCAATCATTCCGGGGAT
CCGTCGACC-3' (for *rodZ*155<>*aph*). The resulting fragments were recombined with the chromosome of TB10/pCX16 and recombinants were selected at 30°C on LB agar supplemented with 50 μg/ml Spec and 25 μg/ml Kan.

For FB60 and FB61 strains, FB58/pCX16 and FB59/pCX16 were transformed with pFB233 [P_{lac}::*rodZ*(1-319)]. Transformants were grown in the presence of 250 μM IPTG and used to prepare P1 lysates. These lysates were subsequently used to introduce the *rodZ*<>*aph* or *rodZ*155<>*aph* allele into strain TB28 harboring various (non-) complementing plasmids.

For FB62/pFB234 [*ispG*<>*aph*/P_{lac}::*ispG*] the *aph* cassette of pKD13 was amplified with primers 5'-
TTTTATCAGAACTAACCAGGTTGCGCGTCTGACCCTCAATGCCGAACAATCACCGGCGCAG
TAAGTGTAGGCTGGAGCTGCTTC-3' and 5'-
TTATTTTTCAACCTGCTGAACGTCAATTCGACGCGCTTCGTCCAGCTGACATTCCGGGGAT
CCGTCGACC-3', and the fragment was recombined with the chromosome of TB10/pFB234. Recombinants were selected at 30°C on LB agar supplemented with 50 μg/ml Amp, 25 μg/ml Kan, and 100 μM IPTG.

Strain FB66 [*yhdE*<>*cat*] was obtained by transduction of *yhdE*<>*cat* from FB57 to TB28.

Strain FB72/pCX16 [*mreB'-rfp-'mreB*/*sdiA*] was obtained by replacement of the *mreB*<>*aph* allele of strain FB1/pCX16/pFB149 [*mreB*<>*aph*/*sdiA*/P_{lac}::*mreBCD*] with the *mreB'-rfp-'mreB* gene from plasmid pFB262 [P_{lac}::*mreB'-rfp-'mreB*] by λ red recombineering. To this end, the *mreB'-rfp-'mreB* gene was amplified from pFB262 with primers 5'-
CGACTCTAGACAGCTTTCAGGATTATCCCTTAGTATG-3' and 5'-
GCAAAAGCTTACTCTTCGCTGAACAGGTCGCC-3'. The resulting product was electroporated into competent FB1/pCX16/pFB149 cells that had grown in LB supplemented with 50 μg/ml each of Amp and Spec, and 250 μM IPTG. Cells were outgrown in SOC media at room temperature for 20 minutes and at 30°C for 60. Recombinants were selected at 30°C on LB agar supplemented with 1% glucose and 1% sodium dodecyl sulfate (SDS), which we found to be

lethal for spherical cells. About 90% of the transformants were kanamycin sensitive and rod-shaped, but showed no fluorescent signal in the red channel and most likely resulted from recombination between the chromosome and the *mreB* gene on pFB149. However, the remaining transformants were kanamycin sensitive rods that showed fluorescent signal in the red channel, indicating they had undergone the desired recombination event. This was verified by PCR analyses as described in the text with two recombinants that still harbored pCX16, but had lost plasmid pFB149, and were named FB72/pCX16. Chromosomal DNA was purified from *wt* strain TB28 and FB72/pCX16, using the Masterpure kit (Epicentre) and PCR analyses were performed with primer pairs A (5'-GGTGGATCCTTGAAAAAATTTCGTGGCATGTTTTCCAATGAC-3' [A1] and 5'-GCAAAAGCTTACTCTTCGCTGAACAGGTCGCC-3' [A2]), and B (5'-AGGGCGCATATGGTTTCCAAGGGCGAGGAGGATAACATGGC-3' [B1] and 5'-CGTTCTCGAGTTGCCCTCCCGGCGCACGCGCAGGC-3' [B2]).

To obtain FB74/pCX16 [*mreB'-rfp-'mreB yhdE*<>*cat*/*sdiA*], the *yhdE*<>*cat* recombineering fragment described above (see FB57) was recombined with the chromosome of FB72/pCX16.

Strain FB76 [*mreB'-rfp-'mreB yhdE*<>*cat*], was next obtained by co-transduction of *mreB'-rfp-'mreB* with *yhdE*<>*cat* from FB74/pCX16 into TB28.

To create FB80 and FB81 [P_{BAD}::*rodZ*], the (*aph araC* P_{BAD}) cassette from pTB29 (Bernhardt and de Boer, 2003) was amplified, using primers 5'-AAGTTAGCCTTAGTGAATGTGGGCTTTGTCACGAGCACACAGACATTGTGTAGGCTGGAGCTGCTTC-3' and 5'-AGGTACGTTTAAATGAGAATTGAGATGCCGGTGAACCATCATGCATCGCCGAATTCGCTAGCCC-3', and the fragment was recombined with the chromosome of strain TB10. Recombinants were selected at 30°C on LB agar supplemented with 25 μg/ml Kan and 0.2% arabinose. FB81 was next obtained by transduction of the P_{rodZ}<>(*aph araC* P_{BAD}) allele from FB80 to TB28. Cells were maintained in the presence of 0.2% arabinose.

Strain FB83 [*mreB'-rfp-'mreB yhdE*<>*frt*] resulted from eviction of *cat* from FB76.

To obtain FB84 [*mreB'-rfp-'mreB yhdE*<>*cat* P_{BAD}::*rodZ*], the P_{rodZ}<>(*aph araC* P_{BAD}) allele was transduced from FB80 to FB76. Cells were maintained in the presence of 0.2% arabinose.

For FB85 [*mreB'-rfp-'mreB yhdE*<>*cat rodZ*<>*aph*], the *rodZ*<>*aph* allele was transduced from FB60/pFB233 to FB76. Transductants were selected at 30°C on M9-maltose agar containing 25 μg/ml Kan.

To create FB86(iFB274) [*parS aph*(P_{lac}::*gfp-Δ30-parB*)], pFB274 was first integrated at the *att*HK site of TB28, generating TB28(iFB274). *parS* was then co-transduced with *aph* from CC4713 to TB28(iFB274).

Strain FB87 [*frt araC* P_{BAD}::*rodZ*] resulted from eviction of *aph* from FB81. Cells were maintained in the presence of 0.2% arabinose.

To obtain FB88(iFB274) [P_{BAD}::*rodZ att*Tn7<>*parS aph*(P_{lac}::*gfp-Δ30-parB*)], iFB274 was transduced from TB28(iFB274) to FB87, yielding FB87(iFB274). *att*Tn7<>*parS* was then co-transduced with *aph* from CC4711 to FB87(iFB274). Cells were maintained in the presence of 0.2% arabinose.

For FB89(iFB274) [P_{BAD}::*rodZ parS aph*(P_{lac}::*gfp-Δ30-parB*)], *parS* was co-transduced with *aph* from CC4713 to FB87(iFB274). Cells were maintained in the presence of 0.2% arabinose.

Strain FB90/pTB63 [*mrdAB*<>*aph*/*ftsQAZ*] was obtained by transduction of *mrdAB*<>*aph* from FB38/pTB59 to FB83/pTB63.

For FB91(λFB234) [*ispG*<>*aph*(P_{lac}::*ispG*)], *ispG*<>*aph* was transduced from FB62/pFB234 to TB28(λFB234). Cells were maintained in the presence of 250 μM IPTG.

To obtain FB93/pCX16 [*mreB'-rfp-'mreB mreCD*<>*aph yhdE*<>*cat*/*sdiA*], the *aph* cassette of pKD13 was amplified with primers 5'-
ATCGGATGCAGGCAGGGGAAGTGTCTGTTTACCCTGCCTGGTCTGATACGATAAGTGTAG
GCTGGAGCTGCTTC -3' and 5'-
TCAGCAAGAAAATCCACGGCCAGAGCACCCCATTGACTACACTACTCCAGAATTCCGGGG
ATCCGTCGACC -3', and the fragment was recombined with the chromosome of FB74/pCX16. Recombinants were selected at 30°C on LB agar with 50 μg/ml Spec and 25 μg/ml Kan.

For FB95/pTB63 [*mreB'-rfp-'mreB mreCD<>aph yhdE<>cat*/*ftsQAZ*], FB93/pCX16 cells were transformed with pCH244 [[P_{lac}::*mreBCD*], and a P1 lysate was prepared on a transformant grown in the presence of 250 μM IPTG. This lysate was then used to co-transduce *mreB'-rfp-'mreB* with *mreCD<>aph* and *yhdE<>cat* into TB28.

To create FB101(iFB273) [*mreB'-rfp-'mreB yhdE<>frt rodZ<>aph*(P_{lac}::*gfp-t-rodZ*)], pFB273 was first integrated at the *att*HK site of TB28, generating TB28(iFB273). iFB273 was then transduced from TB28(iFB273) to FB83, yielding FB83(iFB273). The *rodZ<>aph* allele was next transduced from FB60/pFB233 to FB83(iFB273), giving rise to FB101(iFB273). Cells were maintained in the presence of 250 μM IPTG.

The isolation of Rod2352/pFB184 [*rodZ*::EzTnkan/P_{lac}::*sdiA*::*lacZ*] is described below.

For TB99(iFB274) [*att*Tn7<>*parS aph*(P_{lac}::*gfp-Δ30-parB*)], *att*Tn7<>*parS* was co-transduced with *aph* from CC4711 to TB28(iFB274).

REFERENCES TO SUPPLEMENTARY INFORMATION

Addinall, S.G. and Lutkenhaus, J. (1996) FtsA is localized to the septum in an FtsZ-dependent manner. *J. Bacteriol.*, **178**, 7167-7172.

Bendezu, F.O. and de Boer, P.A. (2008) Conditional lethality, division defects, membrane involution, and endocytosis in *mre* and *mrd* shape mutants of *Escherichia coli. J. Bacteriol.*, **190**, 1792-1811.

Bernhardt, T.G. and de Boer, P.A. (2004) Screening for synthetic lethal mutants in *Escherichia coli* and identification of EnvC (YibP) as a periplasmic septal ring factor with murein hydrolase activity. *Mol. Microbiol.*, **52**, 1255-1269.

Bernhardt, T.G. and de Boer, P.A. (2005) SlmA, a nucleoid-associated, FtsZ binding protein required for blocking septal ring assembly over chromosomes in *E. coli. Mol. Cell*, **18**, 555-564.

Bernhardt, T.G. and de Boer, P.A.J. (2003) The *Escherichia coli* amidase AmiC is a periplasmic septal ring component exported via the twin-arginine transport pathway. *Mol. Microbiol.*, **48**, 1171-1182.

Datsenko, K.A. and Wanner, B.L. (2000) One-step inactivation of chromosomal genes in *Escherichia coli* K-12 using PCR products. *Proc. Natl. Acad. Sci. U S A*, **97**, 6640-6645.

de Boer, P.A.J., Crossley, R.E. and Rothfield, L.I. (1988) Isolation and properties of *minB*, a complex genetic locus involved in correct placement of the division site in *Escherichia coli*. *J. Bacteriol.*, **170**, 2106-2112.

de Boer, P.A.J., Crossley, R.E. and Rothfield, L.I. (1989) A division inhibitor and a topological specificity factor coded for by the minicell locus determine proper placement of the division septum in *E.coli*. *Cell*, **56**, 641-649.

de Boer, P.A.J., Crossley, R.E. and Rothfield, L.I. (1990) Central role for the *Escherichia coli minC* gene product in two different cell division-inhibition systems. *Proc. Natl. Acad. Sci. USA*, **87**, 1129-1133.

Defeu Soufo, H.J. and Graumann, P.L. (2005) Bacillus subtilis actin-like protein MreB influences the positioning of the replication machinery and requires membrane proteins MreC/D and other actin-like proteins for proper localization. *BMC Cell Biol.*, **6**, 10.

Flardh, K., Palacios, P. and Vicente, M. (1998) Cell division genes *ftsQAZ* in *Escherichia coli* require distant cis-acting signals upstream of *ddlB* for full expression. *Mol. Microbiol.*, **30**, 305-315.

Furste, J.P., Pansegrau, W., Frank, R., Blocker, H., Scholz, P., Bagdasarian, M. and Lanka, E. (1986) Molecular cloning of the plasmid RP4 primase region in a multi-host-range tacP expression vector. *Gene*, **48**, 119-131.

Geissler, B., Elraheb, D. and Margolin, W. (2003) A gain-of-function mutation in *ftsA* bypasses the requirement for the essential cell division gene *zipA* in *Escherichia coli*. *Proc. Natl. Acad. Sci. U S A*, **100**, 4197-4202.

Gerdes, S.Y., Scholle, M.D., Campbell, J.W., Balazsi, G., Ravasz, E., Daugherty, M.D., Somera, A.L., Kyrpides, N.C., Anderson, I., Gelfand, M.S., Bhattacharya, A., Kapatral, V., D'Souza, M., Baev, M.V., Grechkin, Y., Mseeh, F., Fonstein, M.Y., Overbeek, R., Barabasi, A.L., Oltvai, Z.N. and Osterman, A.L. (2003) Experimental determination and system level analysis of essential genes in *Escherichia coli* MG1655. *J. Bacteriol.*, **185**, 5673-5684.

Gitai, Z., Dye, N.A., Reisenauer, A., Wachi, M. and Shapiro, L. (2005) MreB actin-mediated segregation of a specific region of a bacterial chromosome. *Cell*, **120**, 329-341.

Guyer, M.S., Reed, R.R., Steitz, J.A. and Low, K.B. (1981) Identification of a sex-factor-affinity site in *E. coli* as gamma delta. *Cold Spring Harb. Symp. Quant. Biol.*, **45**, 135-140.

Guzman, L.M., Belin, D., Carson, M.J. and Beckwith, J. (1995) Tight regulation, modulation, and high-level expression by vectors containing the arabinose P_{BAD} promoter. *J. Bacteriol.*, **177**, 4121-4130.

Guzman, L.M., Weiss, D.S. and Beckwith, J. (1997) Domain-swapping analysis of FtsI, FtsL, and FtsQ, bitopic membrane proteins essential for cell division in *Escherichia coli*. *J. Bacteriol.*, **179**, 5094-5103.

Haldimann, A. and Wanner, B.L. (2001) Conditional-replication, integration, excision, and retrieval plasmid-host systems for gene structure-function studies of bacteria. *J. Bacteriol.*, **183**, 6384-6393.

Hale, C.A. and de Boer, P.A.J. (1997) Direct binding of FtsZ to ZipA, an essential component of the septal ring structure that mediates cell division in *E.coli*. *Cell*, **88**, 175-185.

Johnson, J.E., Lackner, L.L. and de Boer, P.A.J. (2002) Targeting of ^{D}MinC/MinD and ^{D}MinC/DicB complexes to septal rings in *Escherichia coli* suggests a multistep mechanism for MinC-mediated destruction of nascent FtsZ-rings. *J. Bacteriol.*, **184**, 2951-2962.

Johnson, J.E., Lackner, L.L., Hale, C.A. and De Boer, P.A. (2004) ZipA Is Required for Targeting of ^{D}MinC/DicB, but Not ^{D}MinC/MinD, Complexes to Septal Ring Assemblies in *Escherichia coli*. *J. Bacteriol.*, **186**, 2418-2429.

Karimova, G., Dautin, N. and Ladant, D. (2005) Interaction network among *Escherichia coli* membrane proteins involved in cell division as revealed by bacterial two-hybrid. analysis. *J. Bacteriol.*, **187**, 2233-2243.

Karimova, G., Ullmann, A. and Ladant, D. (2001) Protein-protein interaction between *Bacillus stearothermophilus* tyrosyl-tRNA synthetase subdomains revealed by a bacterial two-hybrid system. *J. Mol. Microbiol. Biotechnol.*, **3**, 73-82.

Kruse, T., Blagoev, B., Lobner-Olesen, A., Wachi, M., Sasaki, K., Iwai, N., Mann, M. and Gerdes, K. (2006) Actin homolog MreB and RNA polymerase interact and are both required for chromosome segregation in *Escherichia coli*. *Genes Dev.*, **20**, 113-124.

Kruse, T., Moller-Jensen, J., Lobner-Olesen, A. and Gerdes, K. (2003) Dysfunctional MreB inhibits chromosome segregation in *Escherichia coli. EMBO J.*, **22**, 5283-5292.

Lackner, L.L., Raskin, D.M. and de Boer, P.A. (2003) ATP-dependent interactions between *Escherichia coli* Min proteins and the phospholipid membrane in vitro. *J. Bacteriol.*, **185**, 735-749.

Li, Y., Sergueev, K. and Austin, S. (2002) The segregation of the *Escherichia coli* origin and terminus of replication. *Mol. Microbiol.*, **46**, 985-996.

Liu, Q., Li, M.Z., Leibham, D., Cortez, D. and Elledge, S.J. (1998) The univector plasmid-fusion system, a method for rapid construction of recombinant DNA without restriction enzymes. *Curr. Biol.*, **8**, 1300-1309.

Marblestone, J.G., Edavettal, S.C., Lim, Y., Lim, P., Zuo, X. and Butt, T.R. (2006) Comparison of SUMO fusion technology with traditional gene fusion systems: enhanced expression and solubility with SUMO. *Protein Sci.*, **15**, 182-189.

Mengin-Lecreulx, D., Ayala, J., Bouhss, A., van Heijenoort, J., Parquet, C. and Hara, H. (1998) Contribution of the Pmra promoter to expression of genes in the *Escherichia coli mra* cluster of cell envelope biosynthesis and cell division genes. *J. Bacteriol.*, **180**, 4406-4412.

Mossessova, E. and Lima, C.D. (2000) Ulp1-SUMO crystal structure and genetic analysis reveal conserved interactions and a regulatory element essential for cell growth in yeast. *Mol. Cell*, **5**, 865-876.

O'Toole, G.A. and Kolter, R. (1998) Initiation of biofilm formation in *Pseudomonas fluorescens* WCS365 proceeds via multiple, convergent signalling pathways: a genetic analysis. *Mol. Microbiol.*, **28**, 449-461.

Raskin, D.M. and de Boer, P.A.J. (1997) The MinE ring: an FtsZ-independent cell structure required for selection of the correct division site in *E.coli*. *Cell*, **91**, 685-694.

Reddy, M. (2007) Role of FtsEX in cell division of *Escherichia coli*: viability of *ftsEX* mutants is dependent on functional SufI or high osmotic strength. *J. Bacteriol.*, **189**, 98-108.

Soufo, H.J. and Graumann, P.L. (2003) Actin-like proteins MreB and Mbl from Bacillus subtilis are required for bipolar positioning of replication origins. *Curr. Biol.*, **13**, 1916-1920.

Vinella, D., Joseleau-Petit, D., Thevenet, D., Bouloc, P. and D'Ari, R. (1993) Penicillin-binding protein 2 inactivation in *Escherichia coli* results in cell division inhibition, which is relieved by FtsZ overexpression. *J. Bacteriol.*, **175**, 6704-6710.

Wang, X., de Boer, P.A.J. and Rothfield, L.I. (1991) A factor that positively regulates cell division by activating transcription of the major cluster of essential cell division genes of *Escherichia coli*. *EMBO J.*, **10**, 3363-3372.

Yu, D., Ellis, H.M., Lee, E.C., Jenkins, N.A., Copeland, N.G. and Court, D.L. (2000) An efficient recombination system for chromosome engineering in *Escherichia coli*. *Proc. Natl. Acad. Sci. U S A*, **97**, 5978-5983.